AAEC/E339

AAEC/E339

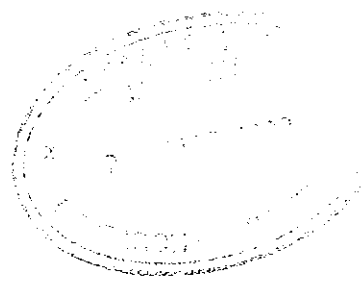

AUSTRALIAN ATOMIC ENERGY COMMISSION

RESEARCH ESTABLISHMENT

LUCAS HEIGHTS

MEASUREMENT OF A MODIFIED RELATIVE CONVERSION RATIO IN MULTI-ROD CLUSTERS

by

P. DUERDEN

September 1975

ISBN 642 99689 X

AUSTRALIAN ATOMIC ENERGY COMMISSION
RESEARCH ESTABLISHMENT
LUCAS HEIGHTS

MEASUREMENT OF A MODIFIED RELATIVE CONVERSION RATIO IN MULTI-ROD CLUSTERS

by

P. DUERDEN

ABSTRACT

An Indo-Australian experiment is described in which relative conversion ratios for a range of UO_2 rod cluster fuel elements in a heavy water moderated reactor were measured using a high resolution Ge(Li) detector to measure directly the neptunium activity following neutron capture in ^{238}U.

The results are compared with calculations made with the UKAEA lattice code WIMS.

National Library of Australia card number and ISBN 642 99689 X

The following descriptors have been selected from the INIS Thesaurus to describe the subject content of this report for information retrieval purposes. For further details please refer to IAEA–INIS–12 (INIS: Manual for Indexing) and IAEA–INIS–13 (INIS: Thesaurus) published in Vienna by the International Atomic Energy Agency.

CAPTURE; CONVERSION RATE; COUNTING TECHNIQUES; ERRORS; FISSION PRODUCTS; FUEL CLUSTERS; FUEL PELLETS; FUEL RODS; HEAVY WATER MODERATED REACTORS; NEPTUNIUM; NEPTUNIUM 239; THERMAL NEUTRONS; URANIUM DIOXIDE

CONTENTS

(continued)

CONTENTS (continued)

1. INTRODUCTION

This report describes one of a series of collaborative projects carried out by the Indian Atomic Energy Commission and the Australian Atomic Energy Commission on the physics of heavy water moderated reactors. The projects have been concerned with measurement and comparison with calculation of particular reactor parameters in fuel clusters containing 7, 19 and 37 14.24 mm diameter natural uranium dioxide rods, with two different spacings and with various coolants in the fuel channels.

Rose, Jain & Menezes (1972) reported an experiment measuring $^{238}U/^{235}U$ fission rate ratios, and Durance & McCulloch (1972) compared the measured values with theoretical predictions. The present report is concerned with measurements of a modified relative conversion ratio and the comparison of these measured ratios with calculated values.

2. DISCUSSION

The conventional conversion ratio in a uranium fuel element is usually defined as the ratio of plutonium production (or ^{238}U capture) to ^{235}U absorption.

It is experimentally convenient to define a *relative conversion ratio* (RCR) comparing the conversion ratio in the fuel element location to that in a thermal neutron spectrum, as

$$RCR = \frac{\left[\frac{^{238}U \text{ capture}}{^{235}U \text{ absorption}}\right]_{\text{fuel element}}}{\left[\frac{^{238}U \text{ capture}}{^{235}U \text{ absorption}}\right]_{\text{thermal}}}$$

which can be rewritten

$$RCR = \frac{\left[\frac{^{238}U \text{ capture}}{^{235}U \text{ fission}}\right]_{\text{fuel element}}}{\left[\frac{^{238}U \text{ capture}}{^{235}U \text{ fission}}\right]_{\text{thermal}}} \times \left[\frac{(1+\alpha) \text{ thermal}}{(1+\alpha) \text{ fuel}}\right]^{235}U$$

$$= R\left[\frac{(1+\alpha) \text{ thermal}}{(1+\alpha) \text{ fuel}}\right]^{235}U$$

where α is the ratio of capture to fission cross sections for ^{235}U and R can be directly determined experimentally using foils enriched and depleted in ^{235}U.

We have measured a slightly different parameter, which we term the

modified relative conversion ratio given by

$$R' = \frac{\frac{^{238}U \text{ capture}}{U \text{ fission}}}{\frac{^{238}U \text{ capture}}{U \text{ fission}}} \quad \begin{matrix} \text{fuel element} \\ \\ \text{thermal} \end{matrix}$$

where U fission now includes the fast fissions of ^{238}U, and can be directly determined using discs of the same enrichment as the fuel elements.

The ^{238}U capture is measured from the resulting ^{239}Np activity and the uranium fission measured by the resulting gross fission product activity.

The measurements were made in clusters of 7, 19 and 37 natural UO_2 rods, each with two different rod spacings. They were arranged in a 3 x 3 lattice in the centre of the ZERLINA reactor (zero power/natural uranium/heavy water). D_2O, H_2O, polystyrene and air were used as the inter-rod 'coolants'. Discs of UO_2 were irradiated for five hours in the clusters and also in a thermal neutron flux.

A high-resolution lithium drifted germanium crystal with associated electronics was used to detect the fission product activity, and γ- and X-rays from the decay of the produced ^{239}Np. The γ- and X-ray spectra resulting from the decay of the ^{239}Np were analytically separated from the general fission product activity and uranium X-ray activity. The accuracy of the experiment was limited by the low activity of the irradiated discs and the removal of the uranium X-ray background spectra from the total spectra resulting from the ^{239}Np decay.

Time restrictions allowed only one set of thermal reference experiments. It would have been preferable to repeat these reference experiments throughout the experimental period as a check on drift of equipment sensitivity for the two different counting techniques.

The measured ratios were compared with calculations made with the Winfrith lattice code WIMS (Askew, Sayers & Kemshell 1966) and the CRAM diffusion code (Hassitt 1962).

3. EXPERIMENTAL ARRANGEMENT

The experiments were made in the zero power/natural uranium/heavy water (100 W) reactor ZERLINA at the Bhabha Atomic Research Centre, Trombay, India. A complete description of ZERLINA is given by Rao *et al.* (1962).

The reactor consists of a cylindrical aluminium tank having an inner diameter of 2286 mm and a height of 4350 mm. A radial graphite reflector 735 mm thick and 3000 mm high surrounds the tank. The bottom graphite reflector is 815 mm thick. Reactivity is controlled by raising or lowering

the D_2O level and the maximum D_2O level allowed for these experiments was 1960 mm. A vertical cross-section of ZERLINA is shown in Figure 1.

The normal core of the reactor consists of 96 natural uranium metal rods 2438 mm long and 35.6 mm diameter forming a lattice with a square pitch of side 190 mm (Figure 2). However, in four of the experiments it was necessary to add 16 ZERLINA fuel rods in peripheral positions so that the reactor could become critical (Figure 3). An experimental *test* region was obtained for assembly irradiations by removing the nine central rods from the core. The fuel cluster in which measurements were to be made was centrally located in this region and surrounded by similar cluster elements to form a 3 x 3 array.

Each cluster consisted of a number of *fuel pencils* (aluminium tubes containing UO_2 pellets). Discs of UO_2, 0.254 mm thick, were irradiated between UO_2 pellets in representative positions of the central cluster. The resulting fission product activity and ^{239}Np activity of the discs were subsequently measured after removal from the reactor.

A thermal column near the effective core boundary (graphite reflector) was created in ZERLINA so that the reference thermal neutron irradiations could take place under similar reactor conditions (start-up period, etc.) to those existing when the experimental discs were being irradiated. Twenty-seven rods were removed from the standard ZERLINA core and a double-walled aluminium thimble was installed in this region. The nearest fuel rod was 880 mm from the thimble. Figure 4 shows the core configuration with the thermal column in the peripheral region.

3.1 UO_2 Pellets and Discs

Forty precision surface ground pellets were manufactured at the same time as fifty discs, nominally 0.254 mm thick. These pellets were always placed adjacent to the discs in the test section and were 14.224 ± 0.005 mm in diameter.

The discs had the same diameter and density as the pellets (10.322 g cm^{-3}). Their thickness was nominally 0.254 mm implying a bulk weight per disc of 0.41661 g. In fact, disc masses varied from 0.35069 to 0.46569 g with a mean of 0.39369 g.

Another 30 surface-ground pellets, density 10.3 g cm^{-3}, 14.24 mm in diameter and about 18.0 mm long were used immediately adjoining the measuring positions. The rest of the test zone fuel was 10.3 g cm^{-3} UO_2 pellets of various lengths and lower surface quality.

3.2 The Experimental Clusters

Clusters of 7, 19 and 37 rods with rod centre-to-centre spacing of ~17 mm

and of ~24 mm were studied. The rod spacing was set by the cluster end-plates. Spacer plates of similar dimensions and the same accuracy as the end-plates were placed at positions along the clusters to prevent bowing. Figure 5 shows the end-plates used in the different experiments.

The outer 8 clusters were the same length (2440 mm) as the normal ZERLINA fuel elements; the centre one was only half this length. This reduced length was not expected to produce any perturbation at the centre measuring position. It enabled the central cluster to be positioned so that the test discs were at the maximum flux position which depended on the critical height of the reactor, and varied from experiment to experiment.

The central cluster could be easily removed from the reactor and quickly dismantled so that the fission product counting of discs could start about four hours after reactor shutdown.

3.2.1 The central cluster

The central cluster was made up of two types of fuel pencils, R pencils containing the experimental discs and UO_2 pellets, and P pencils containing UO_2 pellets only.

The P pencils were 1200 mm aluminium tubes (15.85 mm o.d., 14.38 mm i.d.) filled with the lower quality UO_2 pellets and with fixed threaded plugs Araldited onto both ends. These ends were machined to fit into the bottom and top cluster end-plates where they were fixed by screws.

The R pencils were 1194 mm aluminium tubes (15.83 mm o.d., 15.09 mm i.d.) closed at both ends with removable bayonet plugs. The tubes were loaded with a central test section of UO_2 pellets and discs, and at each end with an encapsulated section of UO_2 pellets. The encapsulated sections consisted of 415 mm, thin-walled aluminium tube (14.79 o.d., 14.36 i.d.) containing the lower quality UO_2 pellets and with 3 mm-thick aluminium plugs Araldited at both ends.

The test section consisted of a thin-walled aluminium tube (14.79 o.d., 14.36 i.d.) with a fixed plug Araldited at one end and a removable bayonet plug at the other (see Figures 6 and 7). The aluminium tube had four longitudinal slots along half its length through which alignment of the experimental disc (with respect to the adjacent pellets) was effected. Two accurately machined pellets and a UO_2 disc were loaded at the half-way position. One of the other machine-ground pellets was placed on either end, and the remaining part of the test section was filled with the lower grade pellets. A bayonet fitting plug was fixed at the open end of the tube and a screw inserted through the fixed plug was tightened very gently until all

the space in the test section was completely filled making no axial movement of either disc or pellet possible. The closeness of fit of the test section within the R pencil did not allow any sideways movement of the disc with respect to the adjacent pellets.

The R pencils were placed in representative positions in different rings of the cluster. Details of the fuel pencils and assembly of a 7-rod cluster are shown in Figure 8.

3.2.2 The outer clusters

These were made up in a similar manner to the central cluster, but used 2440 mm P pencils.

3.2.3 Cluster housing tubes

Clusters were housed in aluminium tubes of dimensions shown in Table 1. These tubes were permanently closed at one end and could be sealed at the other end.

3.2.4 Coolant

H_2O, D_2O, air and expanded polystyrene foam were used in different experiments to represent the 'coolant' filling the housing tubes. The polystyrene $(C_8H_8)n$ was used at a density of about 0.45 g cm^{-3} to simulate 2-phase water/steam coolant. The hydrogen atom concentration is then about 2.08×10^{22} cm^3. Moulding of the polystyrene was successfully carried out to very close tolerances (± 0.04 mm) using techniques described by Rose (1970). Mouldings were manufactured for all but the 37 wide-spaced cluster. Seven mouldings were used in the central experimental cluster and eight in each of the outer eight clusters (see Figure 9 and Table 2).

The clusters were assembled and connected to an extension rod before being sealed in the housing tube (Figure 10). For water-cooled clusters the water level in the tube was set and monitored using a transistorised level indicator (Figure 11). A complete test assembly in its housing tube is shown being loaded into ZERLINA in Figure 12.

3.3 Thermal Neutron Reference Experiments

Two holders were available for the location of the reference foils and discs in the thermal reference thimble. One of the holders was a Perspex cylinder (200 mm length, 38 mm diameter) having a recess (2 mm depth, 18 mm diameter) at either end; the other was a Perspex strip (117 mm length, 40 mm width, 3 mm thickness) having five holes (16 mm diameter, 2 mm depth, 17 mm centre-to-centre) to keep the foils in their locations. The value of the epithermal index $r\sqrt{\frac{T}{T_o}}$ in the thermal reference thimble was found from cadmium

ratio measurements using pure indium foils (thickness 93.4 mg/cm^2) irradiated under a 0.030" (~ 0.8 mm) thickness of cadmium (S.L. Mehta 1970).

The $r\sqrt{\frac{T}{T_o}}$ values were obtained using the relationship of Bigham (1961),

$$r\sqrt{\frac{T}{T_o}} = \frac{G_{th}\,(1 - h\,R_{cd})}{(FR_{cd} - 1)\,\frac{G_r S_o}{g} + R_{cd}\,(1/K - W)}$$

where R_{cd} is the ratio of total to cadmium-covered activity;

G_{th}, G_r are the self-shielding factors in the detector foils for thermal and resonance neutrons, calculated using the method of Hanna (1961);

S_o, g, r, T are defined by Westcott (1956), (values of S_o and g taken from Westcott (1960));

h, F are the transmission factors of the cadmium filter for thermal and resonance neutrons respectively;

$1/K$ approximates the density fraction of the epithermal neutrons transmitted by the cadmium filter; and

W is the correction for resonance activation in the wing of resonance below cadmium cut-off energy.

For thermal irradiation experiments four UO_2 discs were irradiated on two occasions in the strip and two UO_2 discs on two occasions in the cylinder. $r\sqrt{\frac{T}{T_o}}$ was found to be $(1.12 \pm 0.12) \times 10^{-4}$ in the cylindrical holder and $(2.19 \pm 0.17) \times 10^{-4}$ in the strip holder.

The effective cross section of the UO_2 discs $\hat{\sigma}$ in this reference spectrum was obtained using the method of Westcott (1956) where

$$\hat{\sigma} = g\,\sigma_o + 2r\sqrt{\frac{T}{T_o}} \cdot \frac{\Sigma'}{\sqrt{\Pi}} \quad ,$$

$g.\sigma_o$ is the conventional 1/v cross section, and

Σ' is the reduced resonance integral (calculated for the 0.254 mm UO_2 discs by using the cross section preparation code GYMEA (Pollard & Robinson 1969) and found to be 90 barns).

The effective ^{238}U capture cross section for the 0.254 mm UO_2 discs in the thermal reference facility was found to be

$\hat{\sigma}$ = (2.73 + 0.022) barns (strip) and

$\hat{\sigma}$ = (2.73 + 0.011) barns (cylinder) .

A correction factor of 0.992 or 0.995 was therefore applied to the measured Np activity in the reference thermal neutron spectrum to take account

of the departure of the spectrum from Maxwellian form. The correction to the ^{235}U fission cross section was found to be negligible.

Two enriched uranium foils and some depleted uranium foils were also irradiated in the thermal position to assist identification and analysis of Np activity.

3.4 Counting Equipment

The arrangement of the counting equipment is shown schematically in Figure 13. The lithium drifted germanium detector and its associated pre-amplifier gave a FWHM resolution of 3.5 keV. The amplified pulses were fed either directly into a 512-channel analyser or *via* the single channel analyser/discriminator to a timer/scaler.

Irradiated UO_2 discs were placed in individual holders and remained in the holder for both fission product activity and Np activity counting; no lateral or axial displacement of the disc could occur during the counting period. The holders could be located with accurately reproducible positioning about 2 cm above the crystal surface. At this level the sensitivity of the crystal to a point source from the mean sensitivity was down by about 0.3 per cent at the edge of the disc, and up by about 1.5 per cent at the centre. In the axial direction there was a sensitivity change of about 4 per cent per mm.

4. FISSION PRODUCT ACTIVITY COUNTING PROCEDURE AND ANALYSIS

4.1 Counting Procedure

1.33 MeV γ-rays from a ^{60}Co source were used as a standard. They were amplified to a predetermined amplitude which was set using a 512-channel analyser, by adjustment of the amplifier gain. An energy calibration was then made with standard sources and a pulser was set to an equivalent pulse height of 1.4 MeV. Next the single channel analyser and scaler were connected; the discriminator of the SCA was adjusted until only half the count rate from the pulser was registered by the scaler.

The 1.4 MeV discriminator setting was chosen to be well away from fission activity peaks so that the count rate would be little affected by the expected small drifts in the SCA discriminator setting.

The ^{60}Co pulse height was checked after the experiment for drift that might have occurred over the entire day. The maximum change in pulse height that did occur was 0.3 per cent and this could have resulted in a change of up to 0.8 per cent in the count rate. However, in the majority of cases no detectable drift occurred over the counting period. Fission product counting started about 4 hours after the reactor shutdown and continued for up to 8 hours. The active discs were counted repeatedly during the period 4 to 12

hours after the reactor shutdown in a repeating pattern of three 10-second counts with 3 second intervals.

During the counting sequence the background (air) activity and the activity of discs with similar previous irradiation history to those used in the experiment were also measured.

4.2 Analysis

A reference decay curve was obtained by combining together the counts obtained in the four thermal irradiations in the following way. Exponentials were fitted sequentially to 90 minute sections of the individual disc activities for all the discs irradiated in the four thermal spectrum experiments. Calculated values of the activities at 30-second intervals were obtained from these exponentials for the centre 30-minute region; these values were combined to give a decay scheme for the entire counting period for every disc irradiation. These calculated values were combined by a similar method to give first a decay curve for the four separate experiments and then resultant decay curves for the strip holder and the cylindrical holder.

These curves were found to be identical so were themselves combined to give the final curve and a list of reference values at 30-second intervals from 4 to 12 hours after completion of the irradiations.

The relative fission product activities of all discs irradiated in all experiments were obtained by comparing the individual count rates throughout an experiment with the reference decay curve. This gave an activity ratio for each disc in every experiment; weighted means were found for each disc and values 3σ or more from the mean were rejected (σ being a counting statistical variation only). The number of reject counts was well within counting statistics. In no case was any trend in the ratio observed throughout the counting periods, showing that there was no detectable variation in the fission product decay curve for any of the discs irradiated in the different clusters, even though there would have been some variation in the proportion of ^{238}U fissions to total fissions.

5. NEPTUNIUM ACTIVITY, COUNTING PROCEDURE AND ANALYSIS

5.1 Neptunium Counting

The amplifier was directly connected to the 512-channel analyser. The amplifier settings were adjusted so that peaks from standard sources were always registered in the same analyser channels. The counting started about 36 hours after the reactor shutdown and continued for between 8 and 16 hours. Ten minute counts were taken.

Slightly different analyser settings were used in a few of the earlier experiments. Np activities after the thermal neutron spectrum experiments were measured using both analyser settings.

5.2 Analysis

The activity resulting from the Np decay must be separated from the total activity of the irradiated UO_2 discs. In the disintegration of ^{239}Np about 4 per cent of the β-decay goes to an excited state of ^{239}Pu which emits a 106.1 keV γ-ray followed mainly by either a 228 or a 278 keV γ-ray. These 228 and 278 keV γ-rays have large internal K-conversion coefficients giving rise to plutonium K-L_{111} rays at 99.6 keV and 103.8 keV. These plutonium γ- and X-rays must be distinguished from uranium X-rays of comparable energy which exist at 94.7, 98.4, 111.0 and 114.5 keV. Spectra were recorded from 50 to 200 keV, particular attention being given to peaks in the region of 90 to 113 keV.

5.2.1 Background removal

The first stage in the analysis was the removal of background. Polynomials of first, second and third order and an exponential were least-squares fitted to the data in peak-free regions of the total spectrum. The exponential was found to be the best fit and was used as the method of background removal for each data set.

5.2.2 Unirradiated spectrum

A UO_2 disc with similar irradiation history to the experimental discs, but not irradiated in the particular experiment was counted during every Np counting cycle, making spectra available from many different disc masses with different elapsed times since their previous irradiations. One disc was re-used in an experiment after only 11 days, a few after a period of between 15 and 20 days, and the majority after more than 20 days. Count rates obtained in the regions, 86 to 97 and 106 to 116 keV, were identical (within statistical accuracy) for all discs, independent of mass or elapsed time from last irradiation. Activity in the 97 to 106 keV region, however, was greater for the discs with the more recent pre-irradiations. A standard *unirradiated* spectrum was obtained for the 86 to 97 and 106 to 116 keV regions using all disc measurements, and for the 97 to 106 keV regions using only data from discs with elapsed times greater than 35 days since their previous irradiation.

This unirradiated spectrum was removed from all the irradiated spectra, but a further correction was made for the additional Np activity still present to allow for shorter elapsed times since a previous irradiation. Two

foil activities had to be corrected by 1.7 per cent, one by 1.1 per cent, and a few others by between 0.6 and 0.3 per cent for this effect.

5.2.3 Removal of uranium X-ray spectrum

To enable identification of fission product activity and separation of uranium X-ray activity from the spectra, enriched (90 per cent ^{235}U) foils and depleted (0.04 per cent ^{235}U) uranium metal foils were irradiated in the thermal reference thimble. Unirradiated spectra for each foil had previously been measured.

The enriched foil was placed on the detector and its activity measured with the foil uncovered. Next its activity was measured with a 0.051 mm natural uranium foil above, below and on both sides. The same sequence was repeated replacing the natural metal foils with 0.127 mm natural UO_2 discs. These data were analysed in the same way as those from UO_2 discs by fitting an exponential background to peak-free regions and removing it from each of the spectra. The mean unirradiated spectra were then removed from the respective irradiated spectra.

The irradiated enriched foil spectra before and after removal of the background and unirradiated spectra are shown in Figures 14 and 15. While the abundance of uranium X-rays increases with the addition of natural uranium or UO_2 discs, the general activity of the foil decreases. Spectra obtained in the three cases after removal of the appropriate unirradiated spectra, vary only in total count-rate, and there is no contribution in the spectra at the Np decay energies which decrease when the detector is shielded by natural UO_2 or uranium metal foils. Therefore fission product activity in this region is very small compared to uranium X-ray activity; fission product activity would also be negligible in comparison with the Np activity in the case of the irradiated UO_2 discs. A mean uranium X-ray spectrum was obtained from all experimental data (Figure 15).

This mean uranium X-ray spectrum was normalised to the irradiated UO_2 spectrum at the 94.7 and 111 keV uranium X-ray peaks, and subtracted from the total spectrum to give the Np decay spectrum.

A contribution was expected from the Np decay spectrum in the channels at these uranium X-ray peak energies, but as a fixed proportion of the total Np activity for all irradiations.

5.2.4 Intercomparison of Np activity

Figures 16 and 17 show an example of the irradiated UO_2 spectra and the procedure of background and X-ray activity removal. The disc activities obtained were least-squares fitted to the 2.350 day half-life exponential

decay for ^{239}Np. Individual counts greater than ± 3 σ (σ being the counting statistical variation only) from the fitted curve were rejected. The remaining activities were refitted to the exponential. The number of rejected counts was that expected from counting statistics and no deviation from the 2.350 day half-life was observed. Consequently, the Np activities of all discs could be readily intercompared using this half-life to determine the amplitudes of such fits at a standard time (2200 minutes) after reactor shutdown.

6. NEPTUNIUM ACTIVITY/FISSION PRODUCT ACTIVITY RATIO

The ratios of Np activity to fission product activity were found for each individual irradiation and are listed in Tables 3A and 3B, together with the ratios obtained in the thermal neutron spectrum with the same Np analyser settings (see Section 5.1). Table 3A lists results of the early experiments using the standard Np analyser settings after the detector was redrifted; Table 3B, those of earlier experiments with the initial analyser settings.

Mean values of the ratio for measurements made with both foil holders in the thermal neutron spectrum are shown in Tables 3A and 3B. The same ratio was found with both the holders. The error shown for the mean thermal experimental ratios is that obtained from the distribution of the individual foil measurements. It ranges from 1.1 per cent for the initial analyser settings to 0.8 per cent for the later measurements.

7. ERRORS

A survey was made of possible sources of error in experiment, counting, and analysis.

7.1 Edge and Surface Effects in Detector Discs

De Lange *et al.* (1966) reported on a measurement of the edge effect as a part of their Initial Conversion Ratio (ICR) studies on UO_2 lattices. They concluded that there was no significant edge effect for the 0.127 mm wafers they used. We have assumed that similarly there would be no significant effect.

No chipped discs or pellets were used. Disc and pellet surfaces were such that the discs tended to adhere to the pellet surface. The diameters were matched by precision grinding. The equipment permitted very accurate alignment of discs and pellets for irradiation. Consequently we concluded that errors in our experiments due to these effects were negligible.

7.2 Crystal Sensitivity

Tunnicliffe *et al.* (1963) considered the effects of non-uniformity in detector sensitivity and foil activities. The spatial response variation of

the crystal used in our experiment was similar to that used by Tunnicliffe *et al.* who showed the resulting errors in measured ICRs to be negligible.

7.3 Counting Statistics

Average count-rates were obtained in the measurement of the fission product activity and Np activity for each ring of all the clusters. The ratios of the cluster count-rates to the thermal irradiation count-rates are shown in Table 4 which shows that the maximum fission product count-rate in a cluster experiment was about eight times that in the thermal neutron spectrum experiment and that the Np activity count-rate in the cluster experiments was between three and nine times that in the thermal neutron spectrum experiment.

In the case of the clusters, we had errors in the range

fission product activity 0.1 to 0.4 per cent;

Np activity 0.1 to 0.2 per cent.

For the thermal spectrum, the corresponding errors are

fission product activity 0.3 per cent;

Np activity 0.3 per cent.

7.4 Air Background

This was found to be negligible.

7.5 Natural (and Previous) Activity of the Discs

In the experiment with the lowest fission product activity the correction for unirradiated disc activity varied from 2.8 per cent of the total fission activity at the beginning of the counting period, to 10 per cent at the end of the period.

For the Np activity analysis, the discs irradiated in the reference thermal neutron spectrum required the removal of an unirradiated spectrum amounting to 6 per cent of total activity; this fell to between 1 and 2 per cent of the total activity for the discs irradiated in the various clusters.

The background activities used in both analyses were repeatedly measured, but because no variation in background with disc mass was included we have placed an accuracy of ± 4 per cent on these average count rates.

The resulting errors in the background-corrected count rates would therefore be very low in the cluster experiments and would be at a maximum of ± 0.3 per cent in the Np counting and ± 0.4 per cent at the end of the fission counting in the thermal spectrum experiments.

7.6 Dead-time Losses

Overall dead-time of the counting equipment was of the order of 1 μsec

and the maximum fission product count-rate was of the order of only 2000 counts per second. Therefore, the resulting dead-time corrections were negligible.

7.7 Uranium X-ray Spectrum

The measurement of the uranium X-ray spectrum together with the procedure of fitting and removing this spectrum from the total disc activity to give only Np decay activity, can be regarded as the main sources of error in the experiment.

A displacement of a half-channel could possibly have occurred in fitting the uranium X-ray spectrum to the total spectra, but it was expected that the shift in the lead channel would be compensated for by an equivalent shift in the trailing channel.

For the range of clusters studied, the Np spectrum remaining after removal of the uranium X-ray spectrum, contained between 83 and 85 per cent of the total observed counts. This proportion depended on the cluster and the disc mass, but for individual disc irradiations the proportion of the residual count was repeatable to better than ± 0.3 per cent. In the case of the thermal spectrum, the removed uranium X-ray spectrum was observed to depend on the disc mass and to range from 20 to 33 per cent of the total counts as the disc mass varied from 0.35 to 0.48 gms. The variation of an individual measurement was ± 1.4 per cent.

Error in Np activity was expected to result from any error in the actual X-ray spectrum used in the analysis; but the magnitude of this error was expected to be proportional to Np activity and not to effect the ratio $\frac{\text{(Np activity) cluster}}{\text{(Np activity) thermal}}$.

7.8 Positional Errors

Although it was not possible to derive an estimate of any positional error present in the experiment, the accumulation of the possible errors above is consistent with the variations observed in repeated measurements. Scatter in measurements of the Np/fission product activity ratio at similar cluster positions in the same experiment (or in repeated experiments) corresponds to a standard deviation of about 1.8 per cent (Table 3).

7.9 Systematic Errors

We had intended to check unsuspected sources of systematic errors by using alternative techniques and equipment to measure independently fission product and Np activities of each foil. Unfortunately the available alternative equipment proved prone to very severe random drifts in gain, invalidating

any data obtained with it. Therefore no check for systematic errors present in the experimental method could be made. The tabulated accuracies for the experimental results then are derived solely from the analysis of reproducibility and include no allowance for systematic errors.

8. MODIFIED RELATIVE CONVERSION RATIO (R')

8.1 Methods of Calculating R'

Fundamental mode calculations for each experimental cluster were carried out using the Winfrith lattice code WIMS (Askew *et al.* 1966). The CRAM diffusion code (Hassitt 1962) was used to calculate spectrum distortion at the experimental location arising from the ZERLINA environment. It was found to be significant in some of the lattices. In addition, the WDSN transport code (Green 1967) was used to make a few check calculations of the environment correction.

8.1.1 Fundamental mode calculations

Lattice calculations of a cell corresponding to a horizontal section through the experimental test region were performed using the WIMS code. The system was made critical by a search on radial buckling. The main transport calculation option used was WDSN which requires smearing the cluster into concentric rings. The leakage calculation involved the Benoist three-region option combined with a diagonal transport correction.

WIMS library data options used for the main isotopes were:

- Deuterium - Nuclide No.8002 (which has a potential scattering cross section of 3.4 barns and an effective width model for thermal scattering;
- ^{238}U - Nuclide No.2238.4; and
- ^{235}U - Nuclide No.235.4.

The reaction rate ratios in the critical spectrum in each fuel ring of the cluster were made relative to thermal by dividing by the ratio of ^{238}U captures to ^{235}U fissions for a 30°C Maxwellian spectrum. The value calculated for this ratio from the WIMS data was 0.004816.

An assessment was made of the effect on small differences between the test section and surrounding fuel on the modified relative conversion ratio (R'). In addition to a small difference in the amount of cladding, there was a small unknown difference in fuel density due to the poorer quality of the UO_2 pellets in the surrounding pencils. Calculations of the variations in R' caused by changing the broad group spectrum characteristics of the central cluster to those of the outer fuel with an assumed 2 per cent lower density and more cladding, gave (R'-1) values about 1.1 per cent lower for

all clusters, corresponding to corrections of -0.2 to -0.5 per cent in R'. This small correction due to possible density changes has not been included in the quoted results.

8.1.2 Calculation of the environment correction

The environment correction was calculated using a radial model and both the CRAM and WDSN codes. The general arrangements of the regions used in the calculations are shown in Figure 18.

The central cluster was smeared into four regions similar to the regions used in the WIMS cell calculation. The first region represented the inner ring of fuel pencils; the second the outer ring of pencils; the third included some coolant and the aluminium housing tube; and the fourth was D_2O. The eight outer experimental clusters were smeared into the fifth ring which was further surrounded by a region of smeared ZERLINA core whose outer radius was adjusted to obtain criticality. The outer radii of the D_2O region and of the region where the eight outer experimental clusters were smeared, were chosen to give the correct volumes of the regions.

CRAM diffusion theory calculations were made in seven energy groups (Table 5) using a cell DB^2 absorption to represent the axial leakage corresponding to the measured critical height of the system. All cross sections were obtained from the appropriate WIMS calculations, which allows a different treatment of resonance events for inner and outer fuel pencils in a cluster. The resulting test-region spectrum was then compared with one obtained from a calculation made with a similar model, but with the radius of its smeared cluster region increased from 32 to 60 cm to enable an asymptotic spectrum to be achieved in the central channel.

As expected, deviation from the asymptotic spectrum was found in the central cluster depending on both the spectrum mismatch between the experimental cluster and ZERLINA, and the experimental cluster on diffusion properties. The correction to R' was of the order of a few tenths of one per cent; but for the 19- and 37-rod air spaced clusters, it was an order of magnitude larger, reaching about 6 per cent for the 37 expanded air case. The values are shown in Table 6.

To check the adequacy of diffusion theory to estimate the environment correction, the calculations for the 37 expanded air and 37 normal air clusters were repeated substituting WDSN for CRAM. This decreased the correction factors by a further 0.5 per cent for 37 expanded air and 0.3 per cent for 37 normal air. It was concluded that the differences between corrections obtained from transport and diffusion theories were not

significant.

An assessment was also made of the effect of errors in the calculated diffusion coefficient of the experimental lattice on the environment correction. The calculation of D is most difficult for the expanded air clusters. A change of 5 per cent in D for all groups, changed the correction on the ratio for the 19-expanded air cluster by 10 per cent. Since errors in D are expected to be less than 10 per cent, resulting errors due to environment correction are expected to be ~ 1 per cent or less.

8.2 Experimental Values of R'

Tables 7A and 7B list the experimentally determined ratios (R') of Np/fission product activity in the cluster to Np/fission product activity in the thermal spectrum; the respective calculated values are also shown. An average value of R' has been included in the table; it is a simple rod-weighted average of R' over the cluster rather than a ratio of cluster average Np activity to cluster average fission activity.

The five cluster measurements included in Table 7B are those made with the detector before it was redrifted; the thermal spectrum measurement took place after redrifting. A correction factor for the change of efficiency in the detector has been obtained by comparing calculated and experimental values of average R' for the 7-rod clusters. The corrected experimental values are shown. It is not expected that this correction would introduce an error greater than ~ 1 per cent in R' for the 5 experiments.

8.3 Comparison of Experimental and Calculated Values of R'

It can be seen from Tables 7A and 7B that the average calculated values of R' for the 7-rod clusters, within the accuracy of the experiment, are in agreement with the experimental ratios; the calculated 19-rod cluster ratios are ~ 1.5 per cent lower than experiment and the calculated 37-rod cluster ratios are ~ 4 per cent lower than experiment.

Table 8 shows the variation in R' across clusters for both the experimental results and the WIMS calculations. Marked differences are apparent between the calculated and experimental variations. The calculations overestimate the ratio in the outer rings and underestimate the ratios in the central fuel pencil. In the 37-rod cluster cases, these differences are about 2 per cent and 3 per cent respectively when normalised to the same cluster average value.

9. CONCLUSIONS

The Np activity/fission activity ratios for individual radii of a range of UO_2 cluster fuel elements have been measured to an accuracy of ~ 1

per cent. When combined with thermal column measurements, these give the modified relative conversion ratios to an accuracy of approximately 1.5 per cent.

Differences between the cluster test section in which the measurements were made and the surrounding environment in the reactor, made precise comparisons between theory and experiment difficult, especially for the larger clusters with low density coolants where environmental influences were large. However, a tendency for WIMS to calculate too steep a radial variation of R' through a cluster was clearly demonstrated. WIMS also exhibited a probable tendency to under-predict cluster average R' values as the cluster size increases.

Use of a high resolution (3.5 keV FWHM) Li/Ge detector has been shown to be satisfactory for a direct measurement of Np activity, and offers the advantage of being significantly simpler than the usual coincidence technique. Unfortunately, the intended direct comparison of the two methods was not achieved in these particular measurements, but the direct measurement technique should be capable of very satisfactory precision in a more favourable experimental environment.

10. ACKNOWLEDGEMENTS

Many individuals contributed to this experiment. Mr. G. Robinson assisted in the calculational work and Messrs. G.K. Gubbi and V.A. Cokhale in the experimental work.

The staff of BARC workshops fabricated the cluster components. Members of the Reactor Engineering Division at Trombay operated the ZERLINA reactor and assisted in the disc counting.

Mr. R. Farmer assisted in the manufacture of the polystyrene moulds. Messrs. J. Eberhardt and A.J. Tavendale supplied the germanium detector and preamplifier.

11. REFERENCES

Askew, J.R., Sayers, F.J. & Kemshell, P.B. (1966) - J. Br. Nucl. Energy Soc., 5 (4) 564.

Bigham, C.B., Chidley, B.G. & Turner, R.B. (1961) - AECL-1350.

De Lange, P.W., Bigham, C.B., Green, R.E. & Manuel, T.J. (1966) - AECL-2636.

Durance, G. & McCulloch, D.B. (1972) - AAEC/E236.

Green, C. (1967) - AEEW-R498.

Hanna, G.C. (1963) - Nucl. Sci. Eng. 15 : 325-337.

Hassitt, A. (1962) - TRG (Report) 229.

Mehta, S.L. (1970) - BARC Private Communication.

Pollard, J.P. & Robinson, G.S. (1969) - AAEC/E147.

Rao, A.S., Prabgakar, B.S. & Venkatesh Warlu, (1962) - Nucl. Eng. 7 (72) 10198-292.

Rose, A. (1970) - Nucl. Instrum. Methods. 77 : 1.

Rose, A., Jain, H.M. & Menezes, P.F. (1972) - AAEC/E227.

Tunnicliffe, P.R., Skillings, D.J. & Chidley, B.G. (1963) - Nucl. Sci. Eng. 15 : 268-283.

Westcott, G.H. (1956) - AECL-352.

Westcott, G.H. (1960) - AECL-1101.

TABLE 1

DETAILS OF HOUSING TUBES

	I.D. (mm)	O.D. (mm)
7 Normal	57.1	63.5
7 Expanded	88.0	90.0
19 Normal	88.0	90.0
19 Expanded	124.6	127.0
37 Normal	124.6	127.0
37 Expanded	148.8	152.4

TABLE 2

DETAILS OF POLYSTYRENE MOULDINGS

	Outside Diameter (mm)	Ring Diameter (mm)			Average Weight (gms)	Average Density
7 Normal	56.8	0	17.0		73.0	0.446
7 Expanded	87.78	0	26.0		321.0	0.464
19 Normal	87.78	0	17.2	33.5	142.0	0.443
19 Expanded	123.5	0	23.0	44.5	566.0	0.468

TABLE 3A

THE MEASURED NEPTUNIUM AND FISSION ACTIVITIES

Assembly			Fission Product Activity				Neptunium Activity				$\frac{\text{Neptunium Activity}}{\text{Fission Activity}}$				($\frac{Np}{Fiss.}$ Ratio) $\frac{\text{Cluster}}{\text{Thermal}}$ (R')				Average ($\frac{Np}{Fiss.}$ Ratio) $\frac{\text{Cluster}}{\text{Thermal}}$ (R')			
No. of Rods	Normal or Expanded	Coolant	Centre	Ring 1	Ring 2	Ring 3	Centre	Ring 1	Ring 2	Ring 3	Centre	Ring 1	Ring 2	Ring 3	Centre	Ring 1	Ring 2	Ring 3	Centre	Ring 1	Ring 2	Ring 3
7	N	Air	5.354 5.385	5.965 5.875			1.134 1.151	1.306 1.277			2.118 2.137	2.189 2.173			1.175	1.204			1.171	1.193		
7	N	Air	5.280 5.134	5.677 5.661			1.108 1.096	1.223 1.204			2.098 2.130	2.154 2.126			1.167	1.181						
7	N	D_2O	5.868	6.595 6.629			1.222	1.386 1.388			2.082	2.101 2.093			1.188	1.197			1.188	1.197		
7	N	H_2O	3.929 3.928	4.735			0.8480 0.8468	1.012			2.158 2.156	2.137			1.191	1.180			1.191	1.180		
7	E	D_2O	6.951	7.516			1.511	1.634			2.173	2.174			1.200	1.200			1.209	1.203		
7	E	D_2O	6.863 6.864	7.531 7.776			1.487 1.542	1.662 1.680			2.166 2.246	2.206 2.160			1.218	1.205						
19	N	D_2O	3.414	3.906 3.831	4.536 4.738		0.9123	1.033 1.007	1.190 1.223		2.672	2.644 2.628	2.623 2.581		1.475	1.456	1.437		1.475	1.451	1.433	
19	N	D_2O		3.841 3.872	4.540 4.674			1.003 1.016	1.161 1.225			2.611 2.623	2.557 2.620			1.445	1.429					
19	N	H_2O	2.519 2.597	2.800	3.522 3.750		0.6560 0.6650	0.7306	0.8958 0.9267		2.604 2.561	2.609	2.543 2.471		1.426	1.441	1.385		1.435	1.443	1.384	
19	N	H_2O	2.455 2.694	2.936 2.920	3.725 3.994		0.6487 0.6977	0.7523 0.7368	0.9472 0.9853		2.642 2.589	2.562 2.523	2.542 2.466		1.444	1.404	1.383					
19	E	D_2O	3.561	3.892	4.588 4.480		1.047	1.111	1.276 1.268		2.940	2.854	2.781 2.830		1.623	1.576	1.549		1.623	1.576	1.549	
37	N	Air	1.658 1.654	1.730 1.713	1.850 1.914	2.245 2.359	0.5529 0.5646	0.5834 0.5754	0.6166 0.6251	0.7777 0.8267	3.334 3.413	3.372 3.359	3.332 3.265	3.464 3.504	1.864	1.859	1.822	1.924	1.864	1.859	1.822	1.924
37	N	D_2O	1.723	1.811 1.845	2.134 2.137	2.777 2.565	0.6402	0.6681 0.6873	0.7384 0.7461	0.9412 0.9034	3.715	3.689 3.725	3.452 3.491	3.389 3.522	2.051	2.046	1.917	1.908	2.099	2.062	1.962	1.931
37	N	D_2O	1.561	1.737 1.682	1.929	2.557 2.349	0.6068	0.6437 0.6413	0.7005	0.9054 0.8546	3.887	3.705 3.812	3.631	3.540 3.638	2.146	2.076	2.005	1.953				
37	E	Air	1.210 1.224	1.264 1.300	1.344 1.407	1.534 1.650	0.4713 0.4774	0.4998 0.5086	0.5284 0.5423	0.6325 0.6725	3.895 3.900	3.938 3.912	3.886 3.854	4.125 4.075	2.152	2.167	2.137	2.263	2.142	2.146	2.160	2.300
37	E	Air	1.190 1.209	1.236	1.329 1.277	1.460	0.4590 0.4668	0.4756	0.5177 0.5123	0.6178	3.857 3.861	3.847	3.895 4.011	4.231	2.131	2.124	2.183	2.336				
Thermal Spectrum Expts.	Strip Holder		0.09152	0.09262	0.08209	0.08389	0.1643	0.1669	0.1521	0.1540	1.795	1.802	1.853	1.836								
	Strip Holder		0.09402	0.09345	0.09216	0.08850	0.1663	0.1662	0.1649	0.1626	1.769	1.778	1.789	1.837								
	Cylinder Holder		0.09273	0.1116			0.1679	0.2017			1.811	1.806										
	Cylinder Holder		0.1005	0.09930			0.1805	0.1823			1.806	1.836										
											Mean Strip			1.808 ± 0.011								
											Mean Cylinder			1.813 ± 0.008								
											Mean			1.811 ± 0.008								

Note: All measurements made after the detector was redrifted.
Standard settings of the analyser were used.

TABLE 3B

THE MEASURED NEPTUNIUM AND FISSION ACTIVITIES

Assembly*			Fission Product Activity			Neptunium Activity			Neptunium Activity / Fission Activity			($\frac{Np}{Fiss}$ Ratio) $\frac{Cluster}{Thermal}$ (R')			Average ($\frac{Np}{Fiss}$ Ratio) $\frac{Cluster}{Thermal}$ (R')		
No. of Rods	Normal or Expanded	Coolant	Centre	Ring 1	Ring 2	Centre	Ring 1	Ring 2	Centre	Ring 1	Ring 2	Centre	Ring 1	Ring 2	Centre	Ring 1	Ring 2
7	N	Poly	5.256	6.024 6.172		1.147	1.319 1.353		2.182	2.189 2.192		1.247	1.252		1.251	1.264	
7	N	Poly	5.383	6.105 6.195		1.183	1.360 1.386		2.197	2.227 2.237		1.255	1.275				
7	E	Air	5.990	6.263 6.279		1.353	1.449 1.461		2.258	2.313 2.326		1.290	1.325		1.322	1.348	
7	E	Air	6.460	6.646 6.819		1.532	1.599 1.635		2.371	2.405 2.397		1.354	1.371				
7	E	Poly	4.900	5.745 5.704		1.128	1.294 1.309		2.302	2.252 2.294		1.315	1.299		1.302	1.289	
7	E	Poly	5.471	6.273 6.338		1.260	1.429 1.452		2.302	2.276 2.291		1.314	1.304				
7	E	Poly	5.138	5.965 6.112		1.149	1.319 1.358		2.237	2.211 2.221		1.277	1.265				
19	E	Air	2.855	2.954 2.974	3.390 3.323	0.854	0.885 0.894	1.018 1.013	2.991	2.996 3.006	3.002 3.048	1.709	1.715	1.729	1.709	1.715	1.729
19	E	Poly	2.776	3.987 3.077	3.821 3.859	0.765	0.839 0.839	0.991 0.995	2.756	2.717 2.727	2.593 2.578	1.575	1.557	1.478	1.610	1.580	1.513
19	E	Poly	2.703	2.957 3.060	3.689 3.696	0.778	0.883 0.854	1.005 0.995	2.878	2.817 2.791	2.724 2.692	1.645	1.602	1.547			
Thermal** Spectrum Expts.	Strip Holder		0.09152 0.08209	0.09262 0.08389		0.1594 0.1464	0.1614 0.1490		1.741 1.783	1.742 1.776							
	Strip Holder		0.09402 0.09216	0.09345 0.08850		0.1596 0.1586	0.1572 0.1576		1.696 1.720	1.681 1.780							
	Cylinder Holder		0.09273	0.1116		0.1638	0.1980		1.766	1.774							
	Cylinder Holder		0.1005	0.0993		0.1751	0.1744		1.742	1.756							
									Mean Strip 1.740±0.018								
									Mean Cylinder 1.760±0.006								
									Mean 1.750±0.014								

* *These cluster experiments were carried out before the detector had to be redrifted. Analysis with initial settings.*

** *Similar Np analyser settings, but the thermal experiments were carried out after the redrifting.*

TABLE 4

RELATIVE NEPTUNIUM AND FISSION PRODUCT ACTIVITIES FOR VARIOUS LATTICES

Lattice			Total Fission Product $\frac{\text{Rod}}{\text{Thermal}}$				^{239}Np $\frac{\text{Rod}}{\text{Thermal}}$			
No. of Rods	Normal or Expanded	Coolant	Centre Rod	Ring 1	Ring 2	Ring 3	Centre Rod	Ring 1	Ring 2	Ring 3
7	N	Air	5.43	5.96			6.51	7.26		
7	N	D_2O	6.04	6.80			7.09	8.08		
7	N	H_2O	4.04	4.88			4.92	5.88		
7	N	Poly	5.47	6.30			6.74	7.85		
7	E	Air	6.41	6.69			8.37	8.90		
7	E	D_2O	7.10	7.80			8.81	9.59		
7	E	Poly	5.32	6.19			6.86	7.91		
19	N	D_2O	3.55	3.97	4.76		5.33	5.87	6.98	
19	N	H_2O	2.64	2.95	3.86		3.88	4.29	5.47	
19	E	Air	2.94	3.05	3.46		4.95	5.16	5.90	
19	E	D_2O	3.66	3.78	4.39		6.05	6.28	7.21	
19	E	Poly	2.82	3.14	3.87		4.48	4.88	5.78	
37	N	Air	1.59	1.68	1.84	2.24	3.22	3.38	3.64	4.68
37	N	D_2O	1.69	1.82	2.10	2.63	3.61	3.83	4.18	5.22
37	E	Air	1.23	1.30	1.41	1.54	2.73	2.84	3.39	3.34

TABLE 5

GROUP STRUCTURE FOR THE CALCULATIONS

Group	Energy Boundaries
1	10 - 0.821 MeV
2	821 - 5.53 keV
3	5530 - 48.052 eV
4	48.052 - 4.00 eV
5	4.000 - 0.625 eV
6	0.625 - 0.100 eV
7	0.100 - - eV

TABLE 6

CALCULATED VALUES OF R'

Cluster	WIMS Calculations (R')				Correction for Environment Effect on R'		Cluster	WIMS Calculations (R') Corrected for ZERLINA			
	Centre	Ring 1	Ring 2	Ring 3	Inner Rod %	Outer Ring %		Centre	Ring 1	Ring 2	Ring 3
7NH	1.168	1.165			+ 0.2	+ 0.2	7NH	1.170	1.167		
D	1.158	1.195			+ 0.1	+ 0.1	D	1.159	1.196		
P	1.155	1.187			+ 0.1	+ 0.1	P	1.156	1.188		
A	1.137	1.189			-	-	A	1.137	1.189		
7ED	1.212	1.222			-	-	7ED	1.212	1.222		
P	1.186	1.186			-	-	P	1.186	1.186		
A	1.139	1.221			- 0.2	- 0.2	A	1.137	1.218		
19NH	1.428	1.392	1.349		- 0.2	- 0.2	19NH	1.425	1.389	1.346	
D	1.437	1.416	1.456		- 0.3	- 0.4	D	1.432	1.411	1.450	
19ED	1.555	1.532	1.529		- 0.4	- 0.4	19ED	1.548	1.526	1.523	
P	1.442	1.423	1.406		- 0.4	- 0.4	P	1.436	1.418	1.401	
A	1.451	1.444	1.634		- 2.0	- 2.6	A	1.422	1.415	1.592	
37ND	1.927	1.895	1.822	1.868	- 0.5	- 0.6	37ND	1.917	1.886	1.812	1.856
A	1.812	1.795	1.830	1.965	- 1.5	- 1.9	A	1.786	1.768	1.802	1.928
37EA	2.042	2.030	2.082	2.374	- 5.0	- 6.3	37EA	1.940	1.928	1.978	2.224

TABLE 7A

CALCULATED AND EXPERIMENTAL MODIFIED RELATIVE CONVERSION RATIOS (R')

Cluster	Calculated R'					Experimental R'				
	Centre	Ring 1	Ring 2	Ring 3	Average	Centre	Ring 1	Ring 2	Ring 3	Average
7NA	1.137	1.189			1.181	1.171 ± 0.016	1.193 ± 0.017			1.190 ± 0.017
7ND	1.159	1.196			1.190	1.188 ± 0.017	1.197 ± 0.017			1.196 ± 0.017
7NH	1.170	1.167			1.167	1.191 ± 0.017	1.180 ± 0.016			1.182 ± 0.016
7ED	1.212	1.222			1.220	1.209 ± 0.017	1.203 ± 0.017			1.204 ± 0.017
19ND	1.432	1.411	1.450		1.436	1.475 ± 0.020	1.451 ± 0.020	1.433 ± 0.020		1.441 ± 0.020
19NH	1.425	1.389	1.346		1.364	1.435 ± 0.020	1.443 ± 0.020	1.384 ± 0.020		1.405 ± 0.020
19ED	1.548	1.526	1.523		1.525	1.623 ± 0.022	1.576 ± 0.022	1.549 ± 0.022		1.561 ± 0.022
37NA	1.786	1.768	1.802	1.928	1.857	1.864 ± 0.032	1.859 ± 0.032	1.822 ± 0.032	1.924 ± 0.033	1.879 ± 0.032
37ND	1.917	1.886	1.812	1.856	1.848	2.099 ± 0.036	2.062 ± 0.036	1.962 ± 0.033	1.931 ± 0.033	1.967 ± 0.033
37EA	1.940	1.928	1.978	2.224	2.089	2.142 ± 0.036	2.146 ± 0.036	2.160 ± 0.036	2.300 ± 0.039	2.225 ± 0.038

TABLE 7B

CALCULATED AND EXPERIMENTAL MODIFIED RELATIVE CONVERSION RATIOS (R')

Cluster	Calculated R'				Experimental R'			
	Centre	Ring 1	Ring 2	Average	Centre	Ring 1	Ring 2	Average
7NP	1.156	1.188		1.183	1.251 ± 0.023	1.264 ± 0.023		1.262 ± 0.023
7EA	1.137	1.218		1.206	1.322 ± 0.024	1.348 ± 0.024		1.344 ± 0.024
7EP	1.186	1.186		1.186	1.302 ± 0.024	1.289 ± 0.024		1.291 ± 0.024
19EA	1.422	1.415	1.592	1.527	1.709 ± 0.031	1.715 ± 0.031	1.729 ± 0.031	1.724 ± 0.031
19EP	1.436	1.418	1.401	1.408	1.610 ± 0.029	1.580 ± 0.028	1.513 ± 0.027	1.539 ± 0.028

Derived Efficiency Correction 0.918

Cluster	Calculated R'				Experimental R' Including Efficiency Correction			
	Centre	Ring 1	Ring 2	Average	Centre	Ring 1	Ring 2	Average
7NP	1.156	1.188		1.183	1.148 ± 0.022	1.160 ± 0.024		1.158 ± 0.024
7EA	1.137	1.218		1.206	1.213 ± 0.024	1.237 ± 0.024		1.234 ± 0.025
7EP	1.186	1.186		1.186	1.194 ± 0.024	1.183 ± 0.024		1.185 ± 0.024
19EA	1.422	1.415	1.592	1.527	1.568 ± 0.032	1.573 ± 0.032	1.586 ± 0.032	1.581 ± 0.032
19EP	1.436	1.418	1.401	1.408	1.477 ± 0.030	1.450 ± 0.029	1.388 ± 0.028	1.412 ± 0.028

TABLE 8

VARIATION OF THE CAPTURE/FISSION RATIO ACROSS THE CLUSTER

Cluster	Calculated Capture/Fission				Experimental Capture/Fission			
	Centre	Ring 1	Ring 2	Ring 3	Centre	Ring 1	Ring 2	Ring 3
7NA	0.960	1.010			0.985 ± 0.008	1.000 ± 0.008		
7ND	0.975	1.005			0.990 ± 0.008	1.000 ± 0.008		
7NH	1.005	1.000			1.015 ± 0.008	1.000 ± 0.008		
7NP	0.975	1.005			0.990 ± 0.008	1.005 ± 0.008		
7EA	0.940	1.010			0.980 ± 0.008	1.005 ± 0.008		
7ED	0.990	1.000			1.005 ± 0.008	1.000 ± 0.008		
7EP	1.000	1.000			1.010 ± 0.008	1.000 ± 0.008		
19ND	0.995	0.980	1.010		1.025 ± 0.008	1.005 ± 0.008	0.995 ± 0.008	
19NH	1.045	1.020	0.985		1.020 ± 0.008	1.030 ± 0.008	0.985 ± 0.008	
19EA	0.930	0.930	1.040		0.990 ± 0.008	0.995 ± 0.008	1.005 ± 0.008	
19ED	1.015	1.000	1.000		1.040 ± 0.008	1.010 ± 0.008	0.995 ± 0.008	
19EP	1.020	1.005	0.995		1.050 ± 0.008	1.030 ± 0.008	0.985 ± 0.008	
37NA	0.960	0.955	0.970	1.040	0.990 ± 0.010	0.990 ± 0.010	0.970 ± 0.010	1.025 ± 0.010
37ND	1.035	1.019	0.980	1.005	1.070 ± 0.010	1.050 ± 0.010	0.995 ± 0.010	0.980 ± 0.010
37EA	0.930	0.925	0.950	1.065	0.960 ± 0.010	0.965 ± 0.010	0.970 ± 0.010	1.035 ± 0.010

Normalised to the average capture/fission ratio for the cluster.

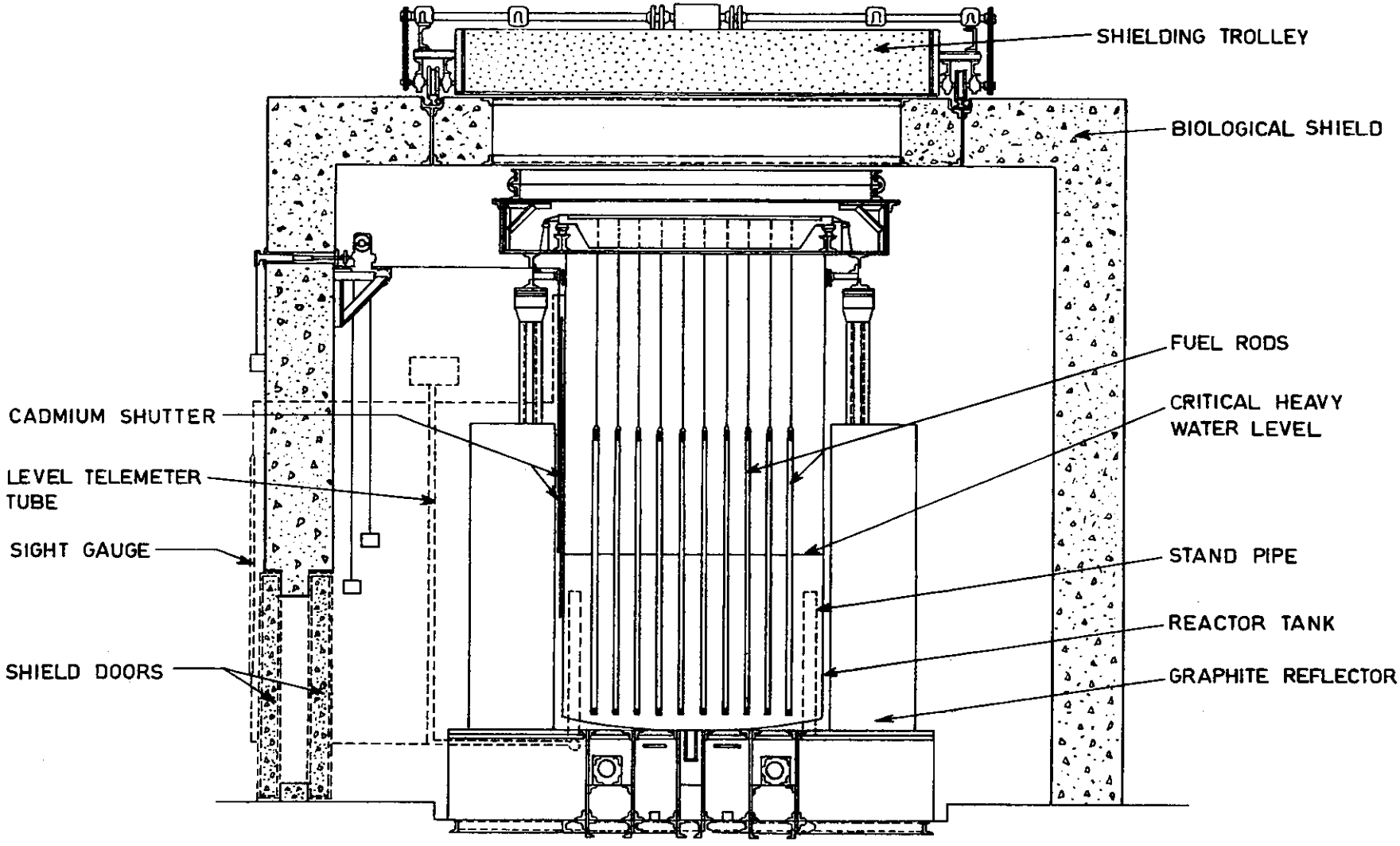

FIGURE 1. VERTICAL CROSS-SECTION OF ZERLINA

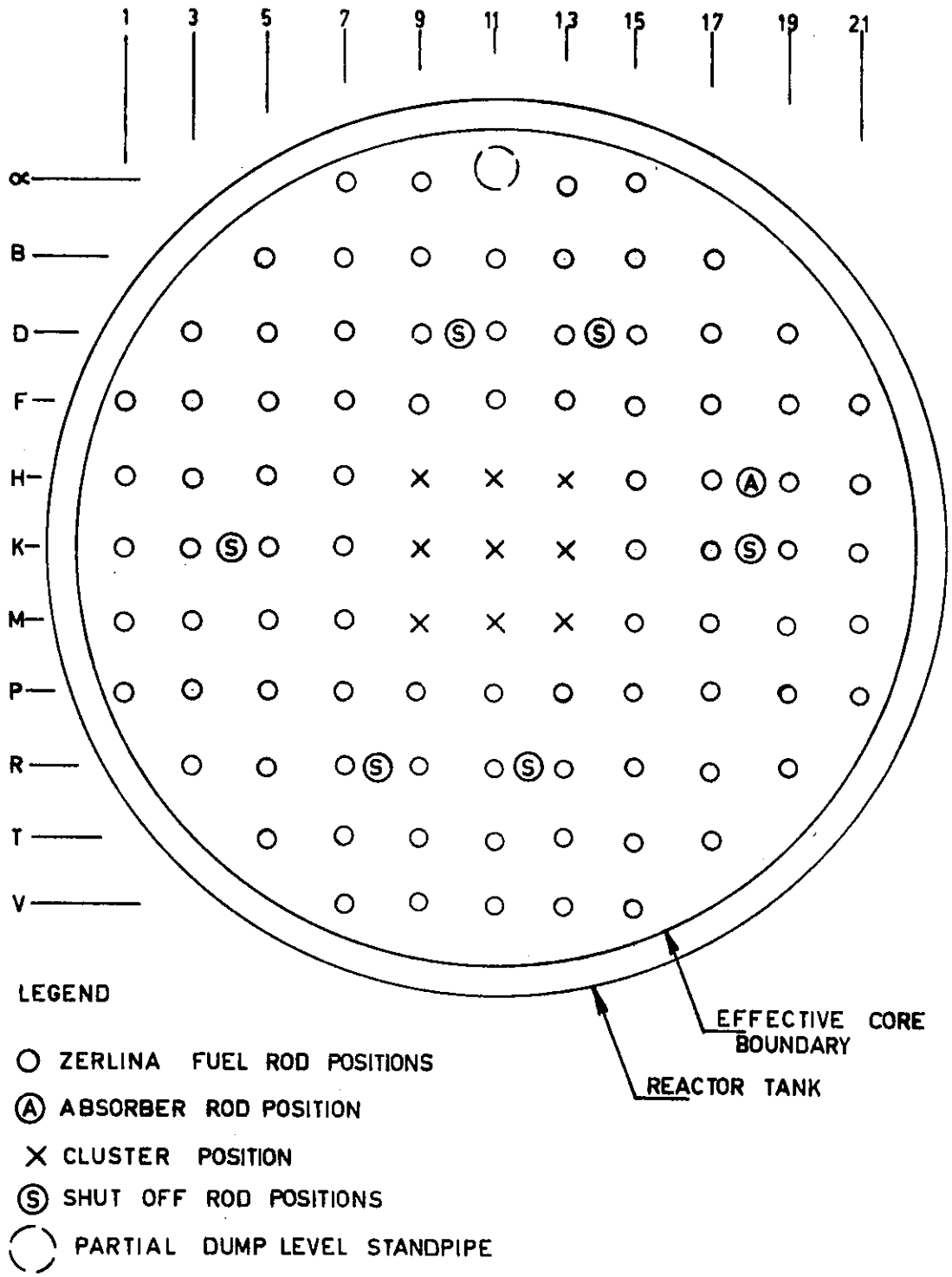

FIGURE 2. ZERLINA - THE CORE ARRANGEMENT FOR THE NORMAL EXPERIMENT

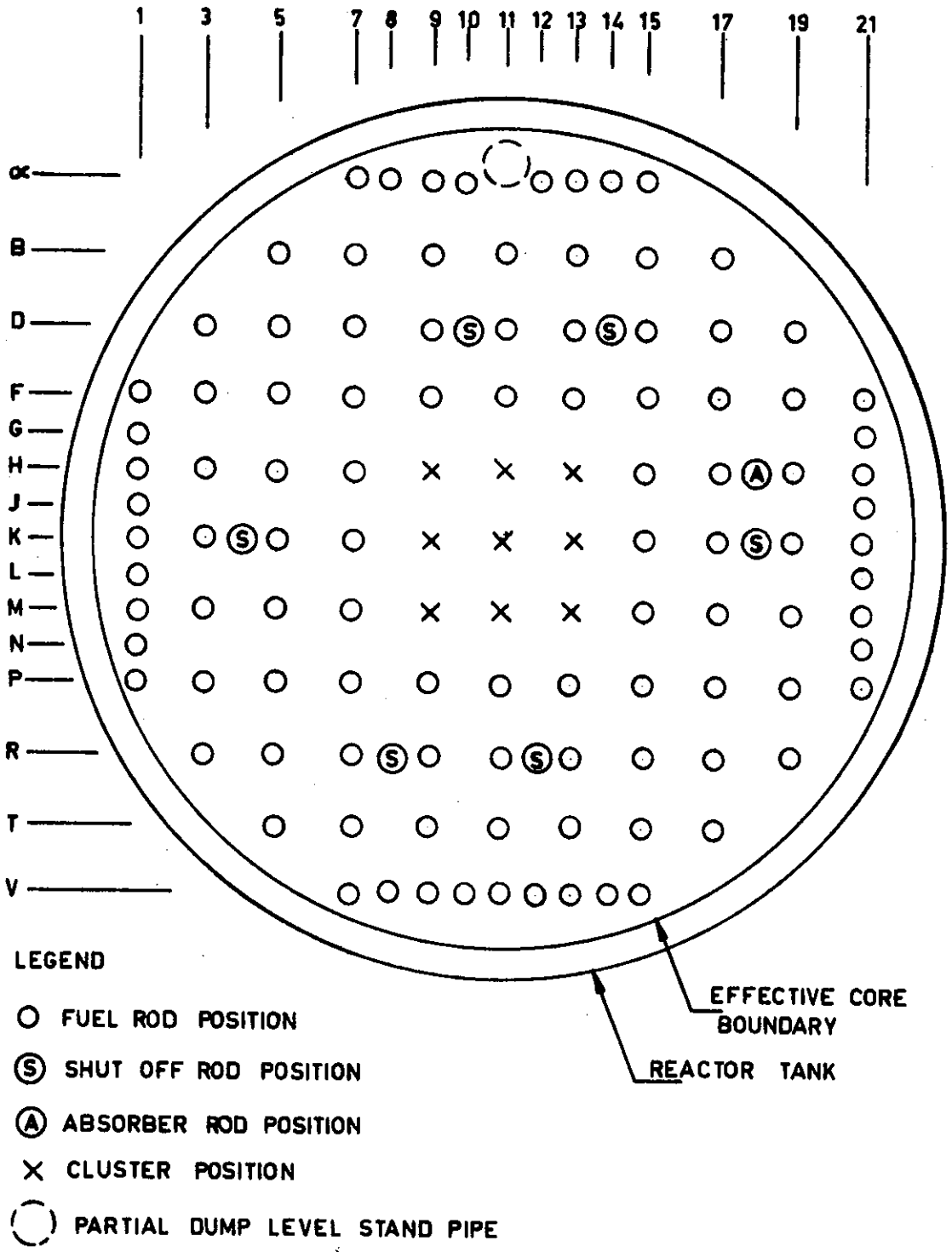

FIGURE 3. ZERLINA - THE CORE ARRANGEMENT WITH THE ADDITIONAL FUEL ELEMENTS

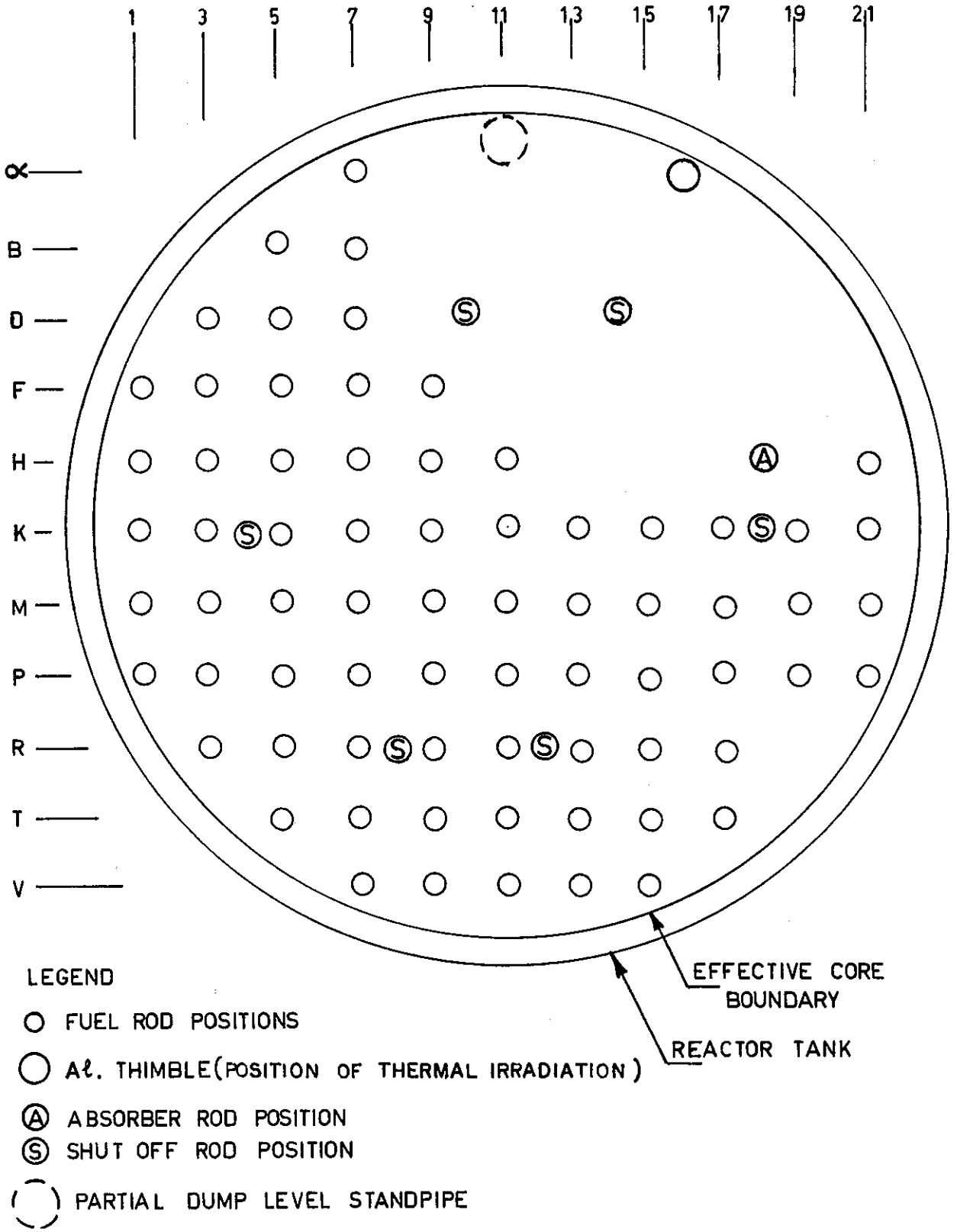

FIGURE 4. ZERLINA - THE CORE ARRANGEMENT FOR THE THERMAL MEASUREMENTS

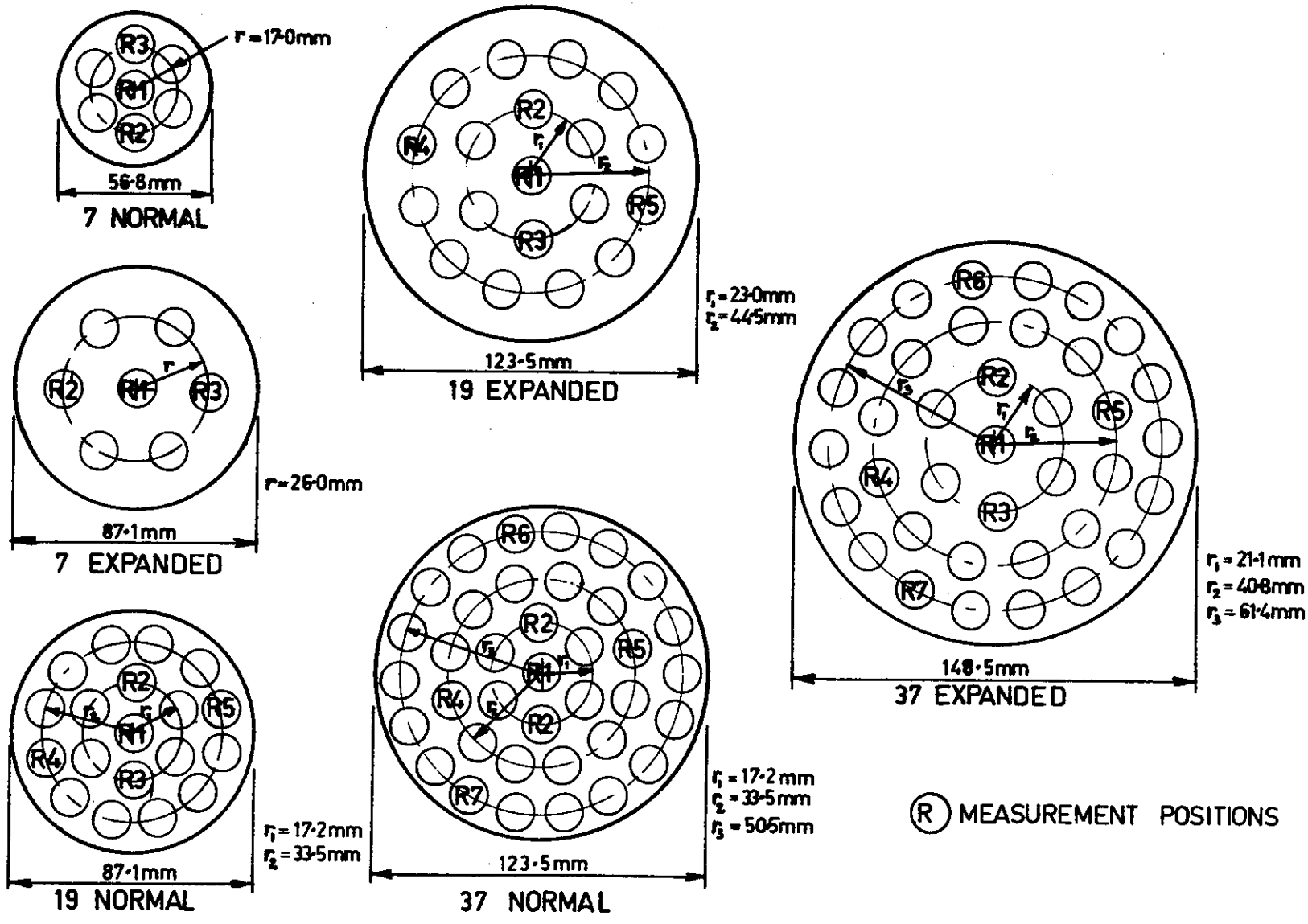

FIGURE 5. CLUSTER DETAILS (END-PLATES)

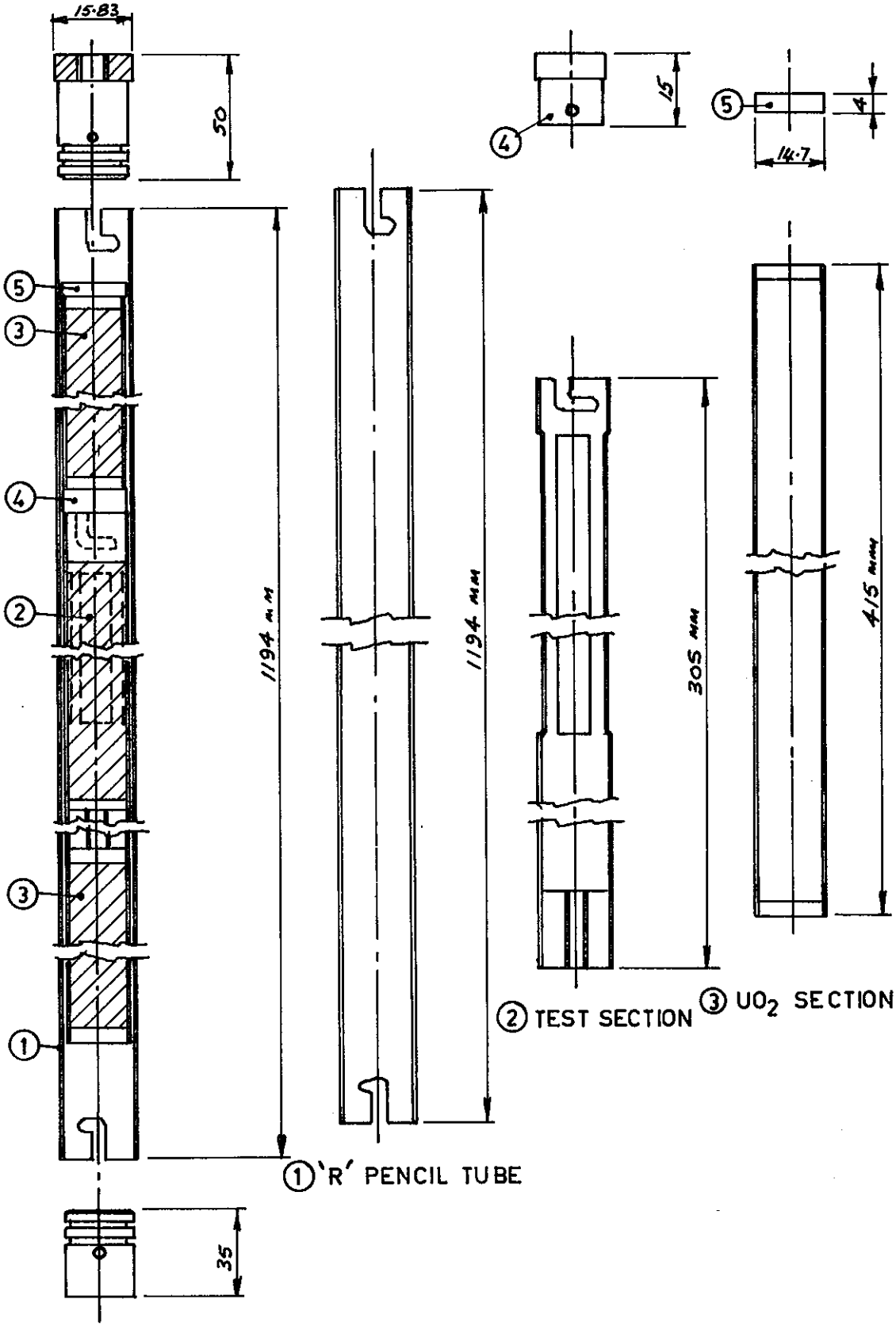

FIGURE 6. TEST SECTION CROSS SECTION

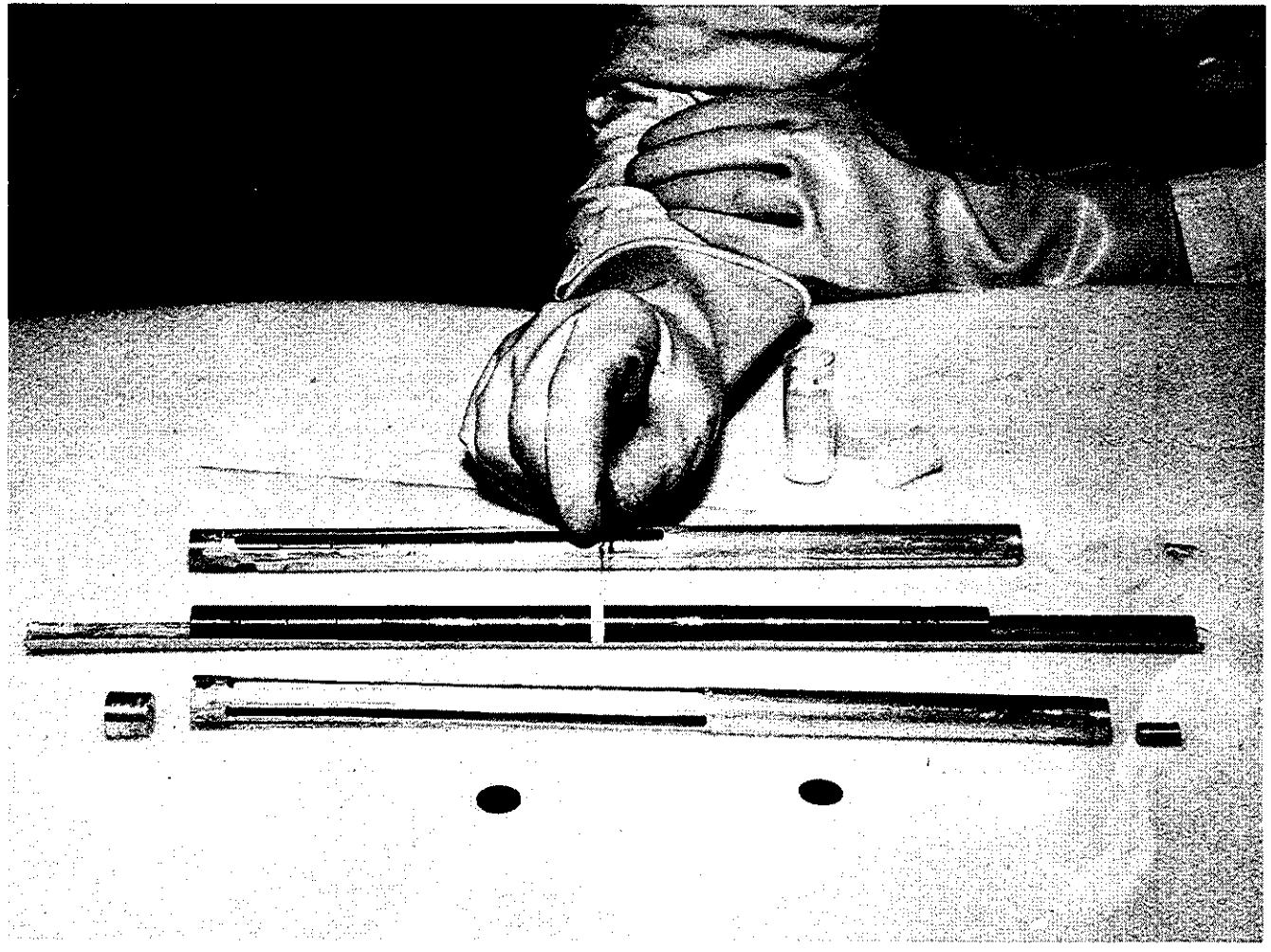

FIGURE 7. THE TEST SECTION

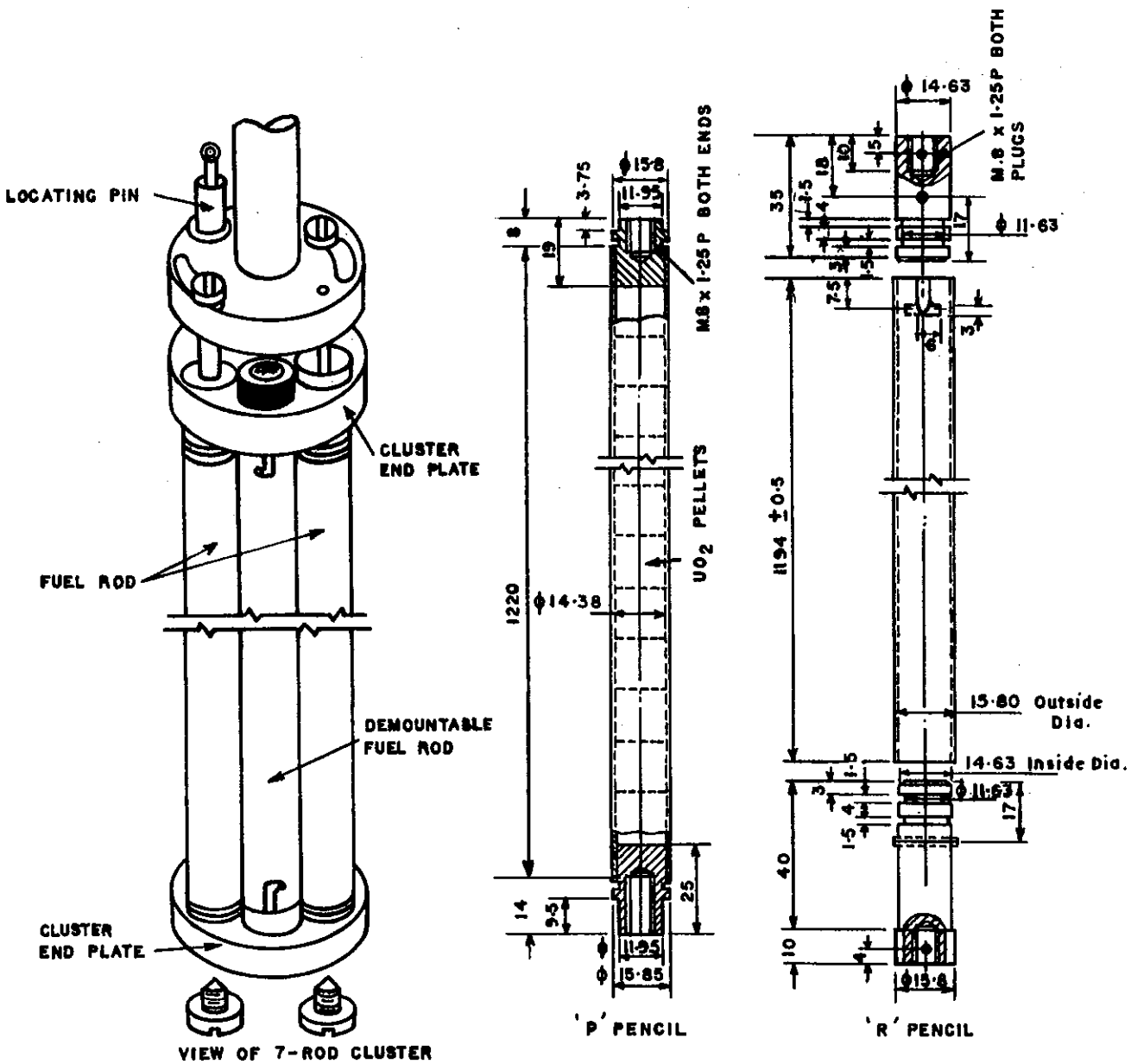

FIGURE 8. DETAILS OF FUEL PENCILS AND ASSEMBLY OF 7-ROD CLUSTER

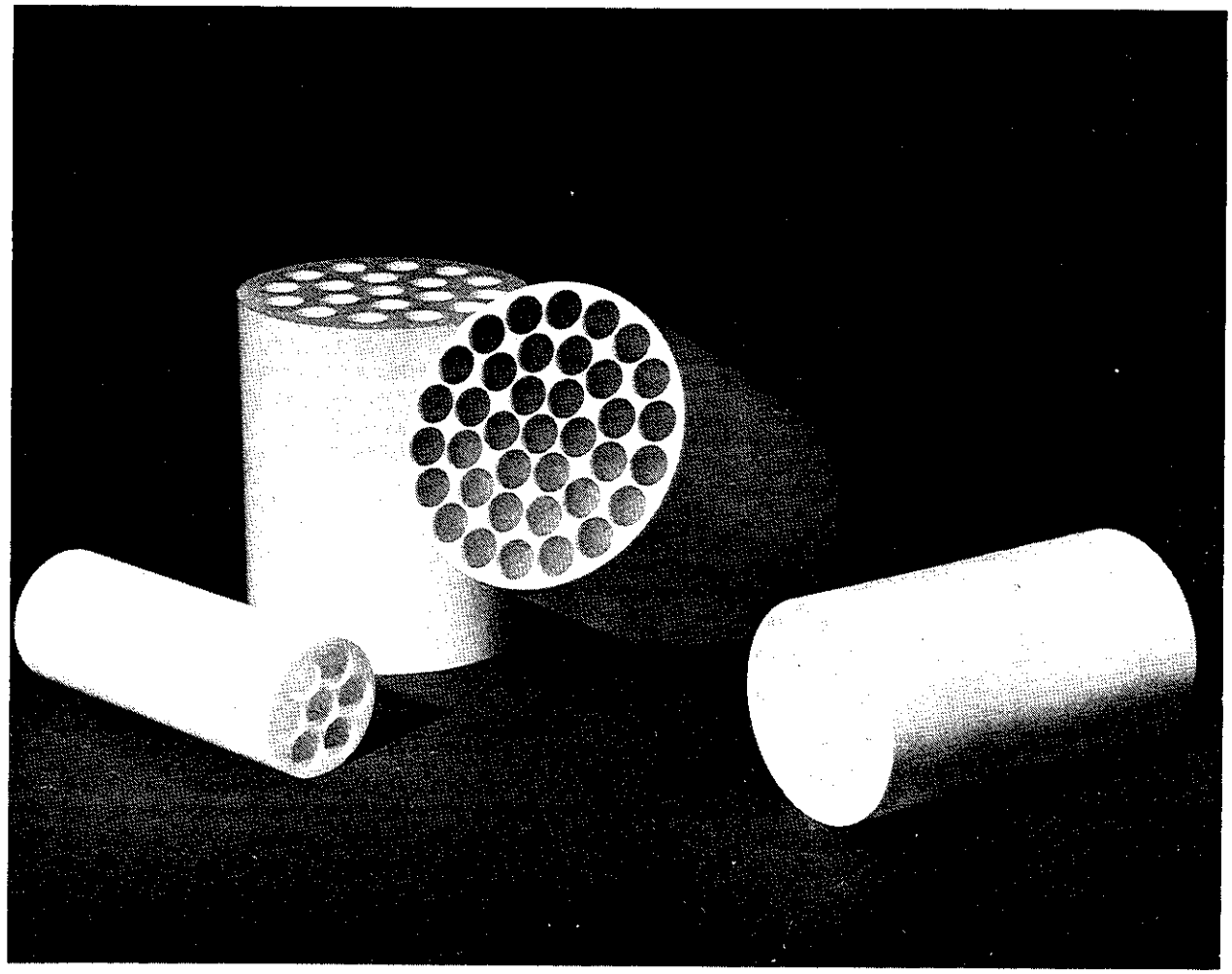

FIGURE 9. POLYSTYRENE MOULDINGS USED IN THE EXPERIMENTS

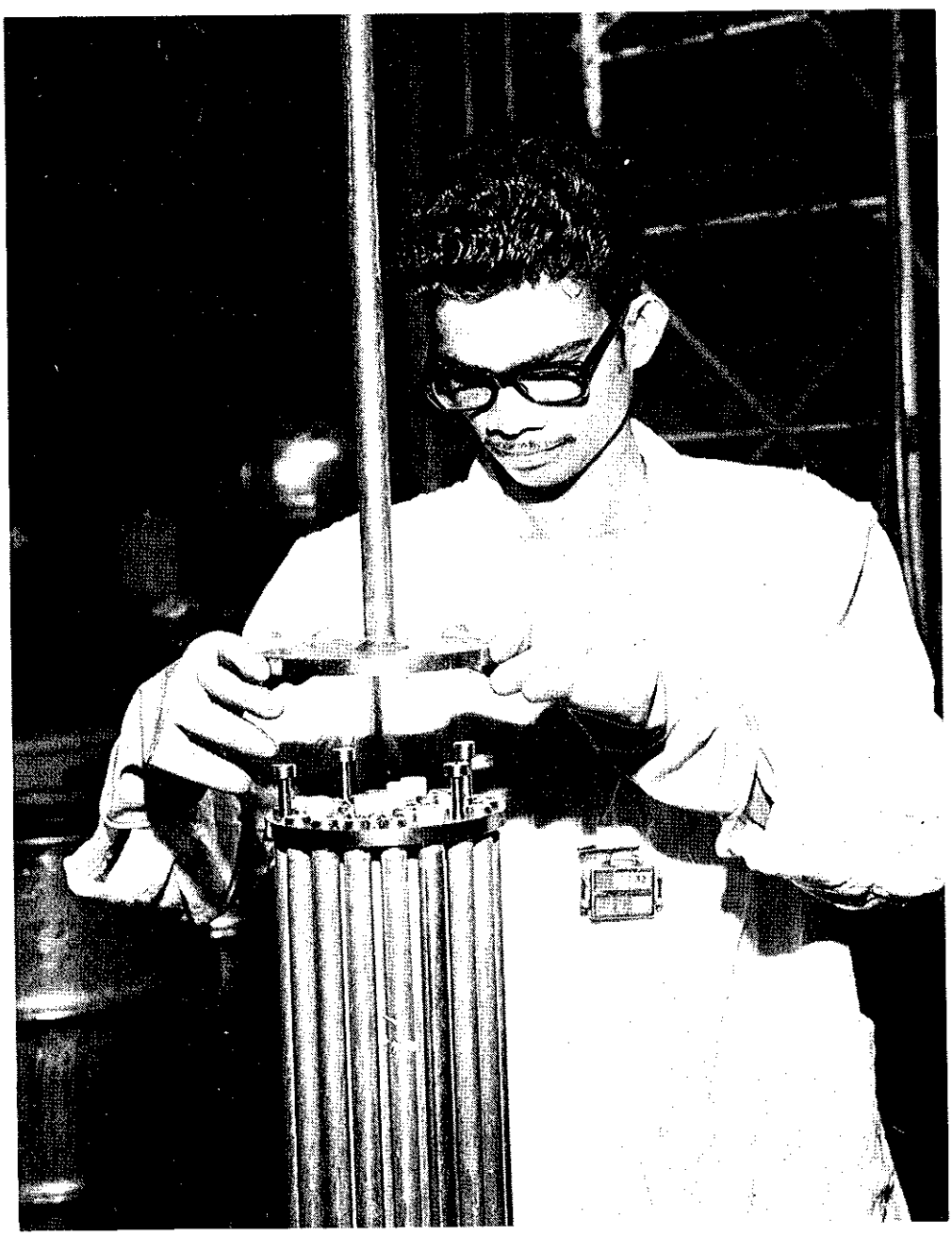

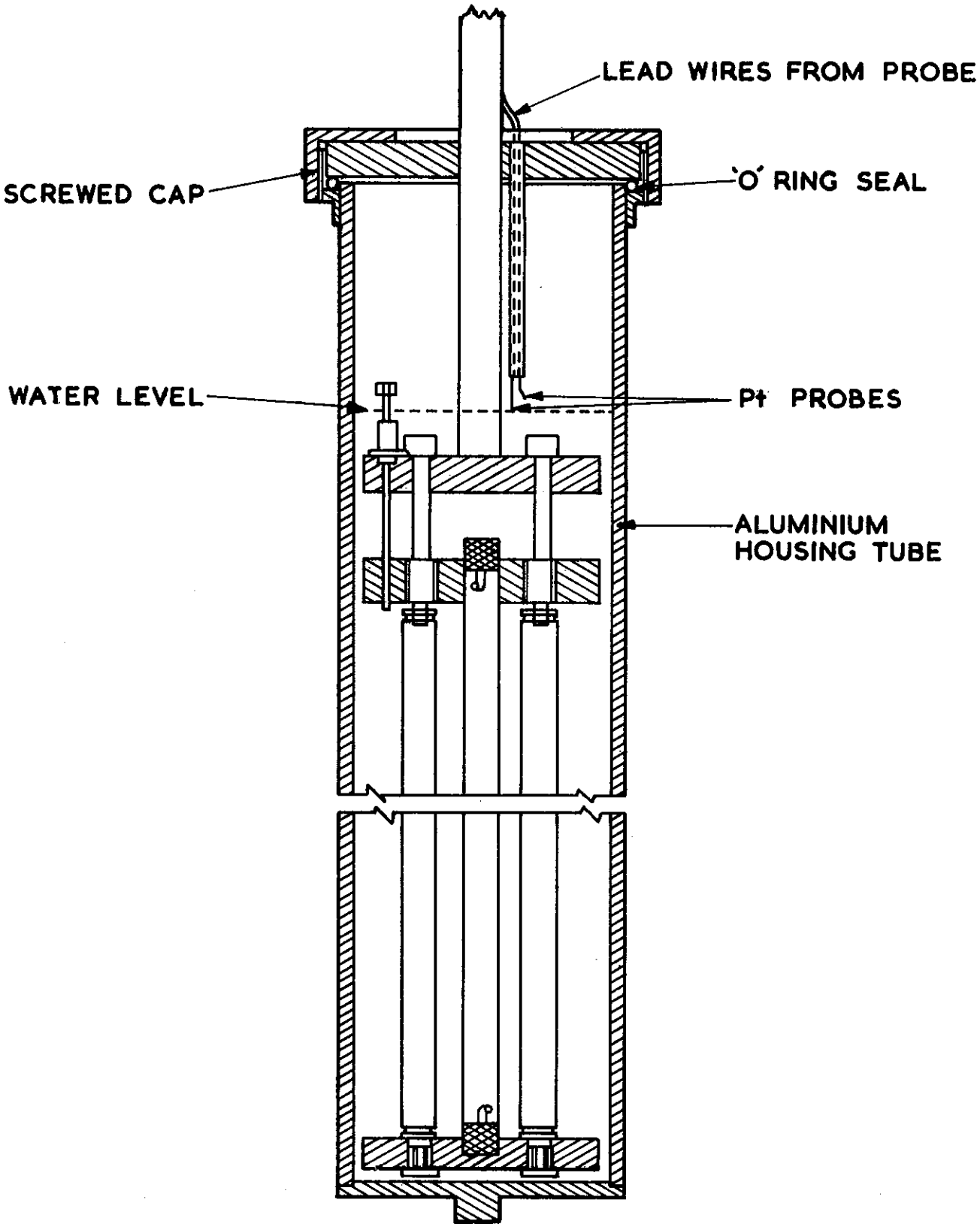

FIGURE 11. SECTION OF COMPLETE 7-ROD CLUSTER IN HOUSING TUBE

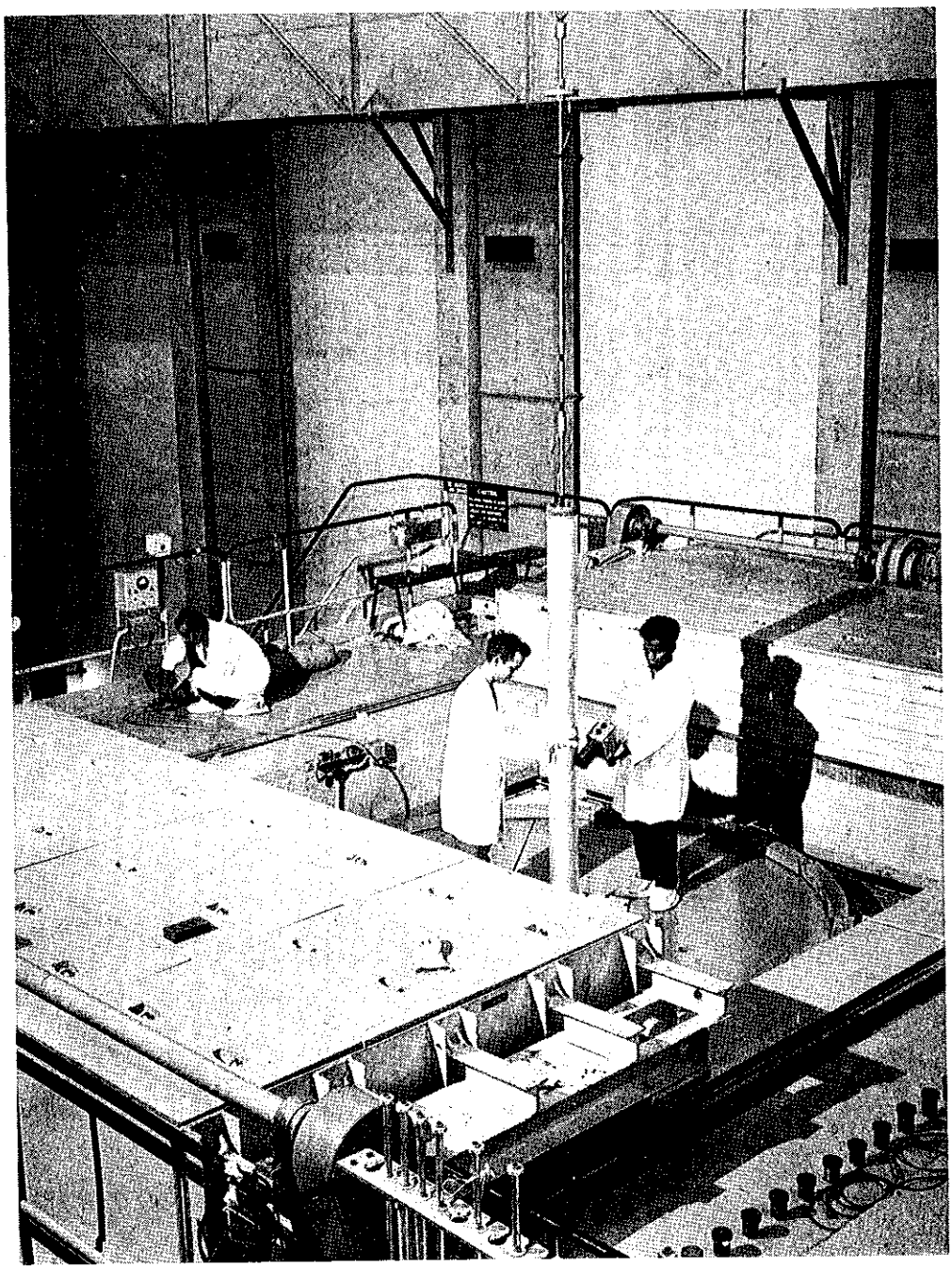

FIGURE 12. A COMPLETE CLUSTER ASSEMBLY BEING LOADED INTO ZERLINA

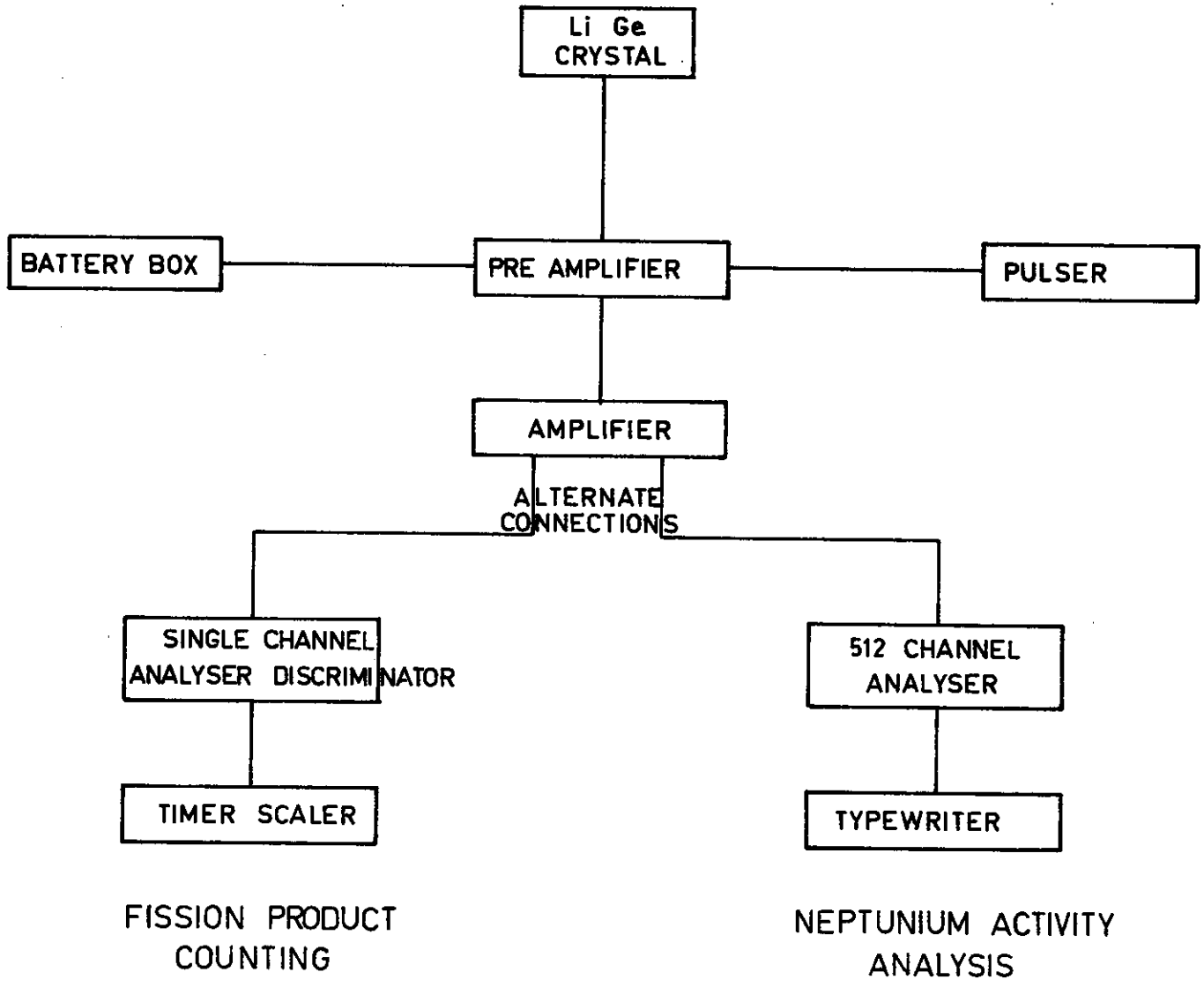

FIGURE 13. BLOCK DIAGRAM OF THE COUNTING EQUIPMENT

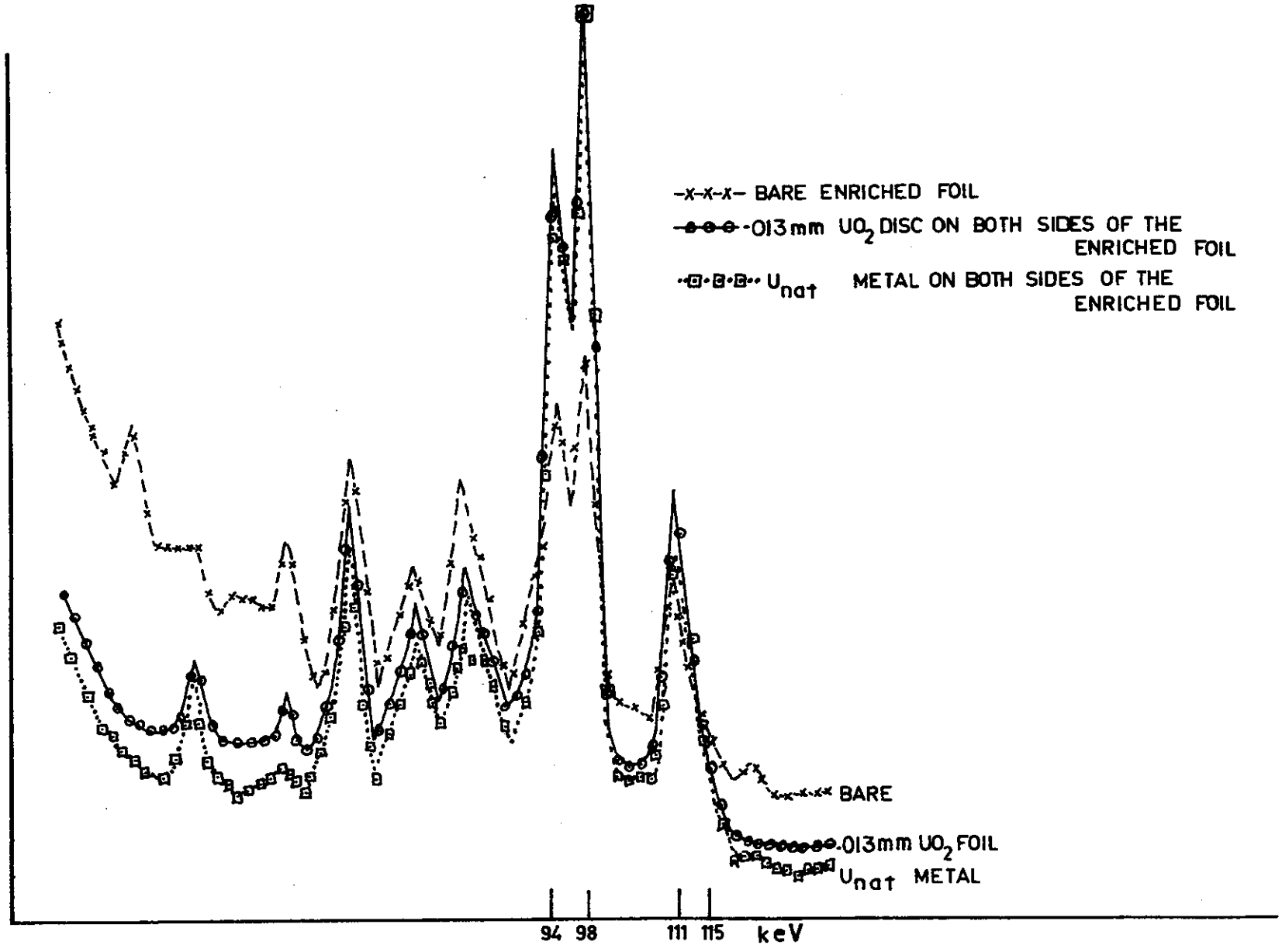

FIGURE 14. SPECTRA OF THE IRRADIATED ENRICHED ^{235}U FOIL

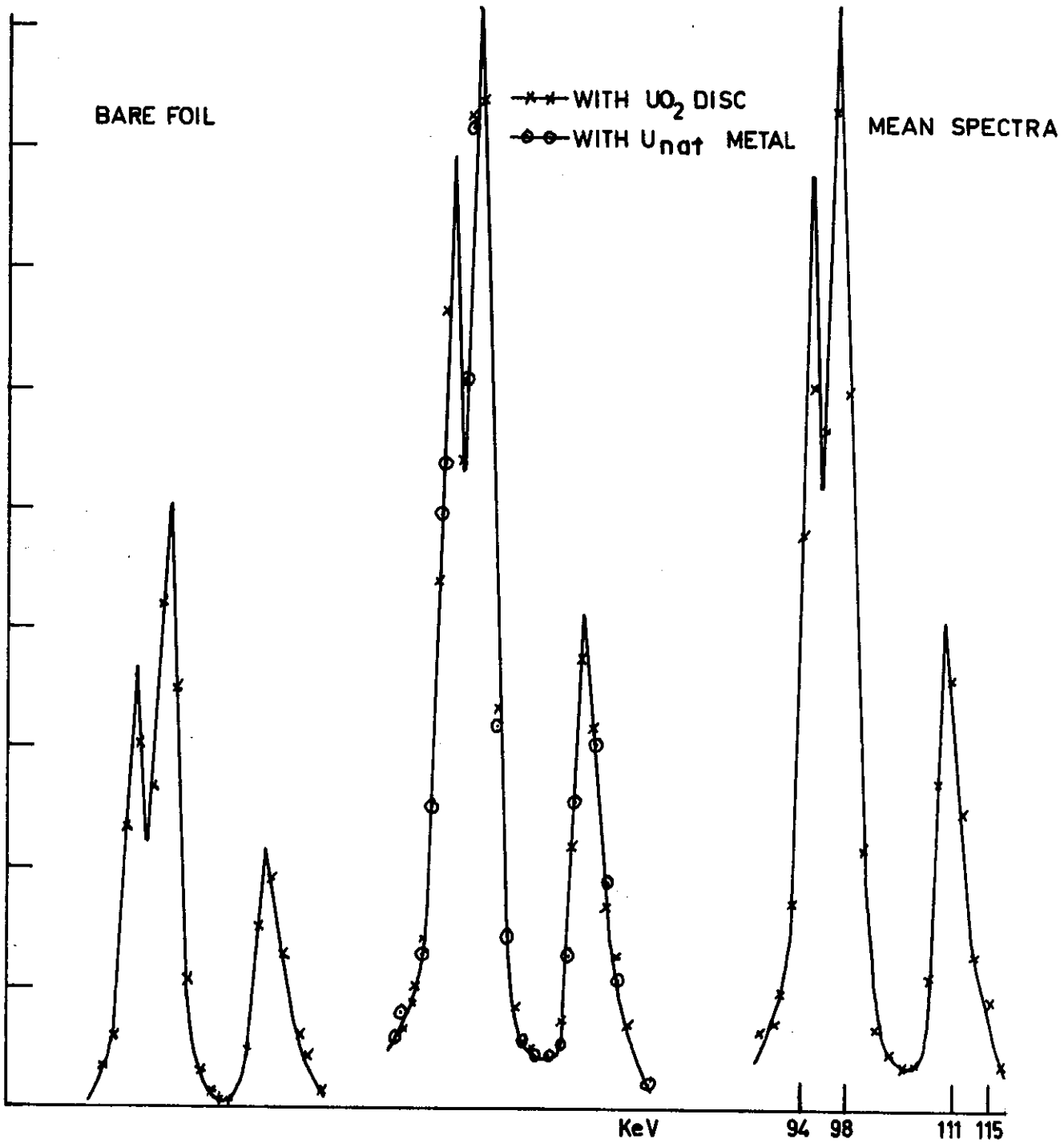

FIGURE 15. THE ANALYSIS OF THE SPECTRA FROM THE ENRICHED ^{235}U FOIL

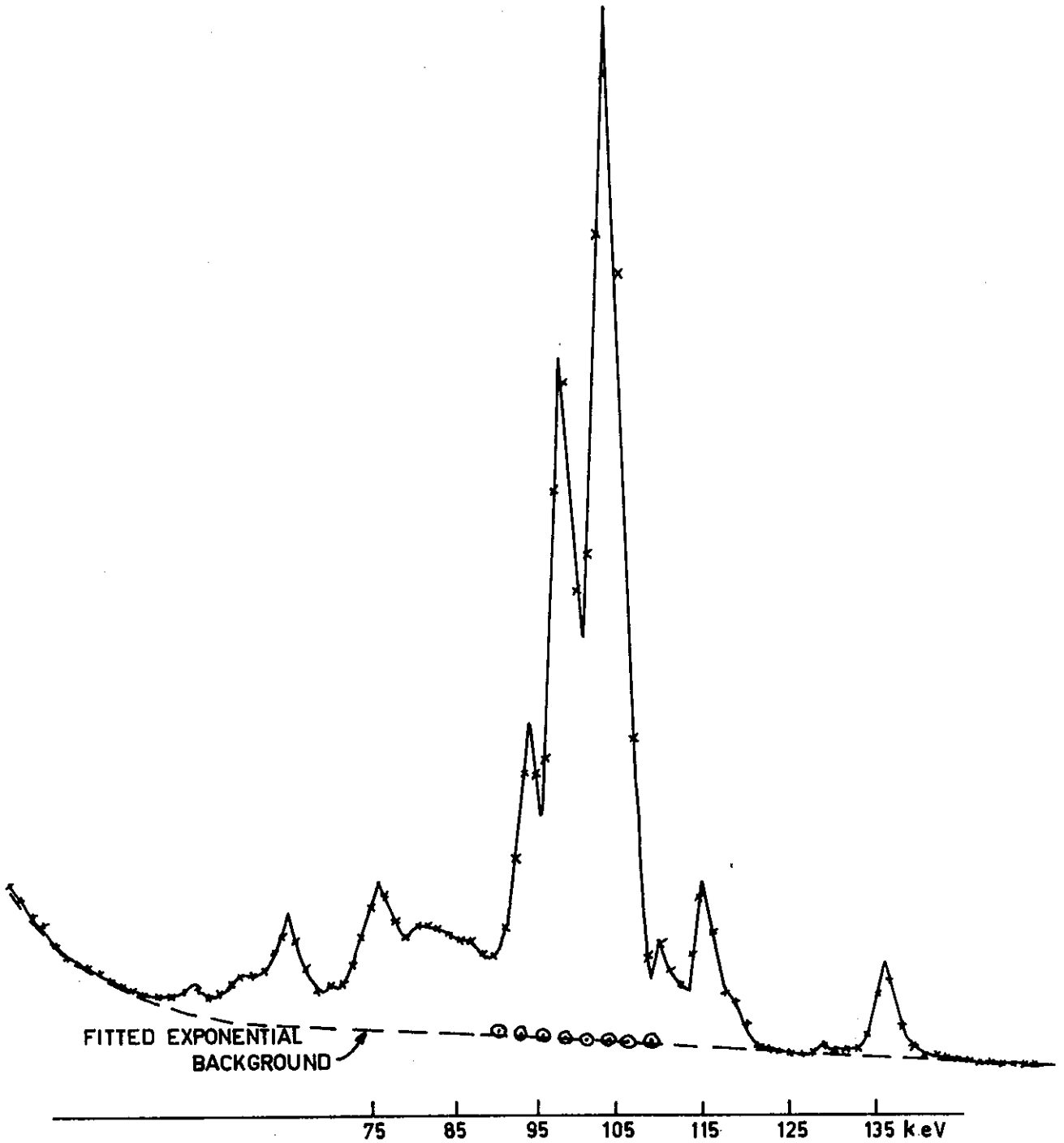

FIGURE 16. THE SPECTRUM OF THE IRRADIATED UO_2 DISC

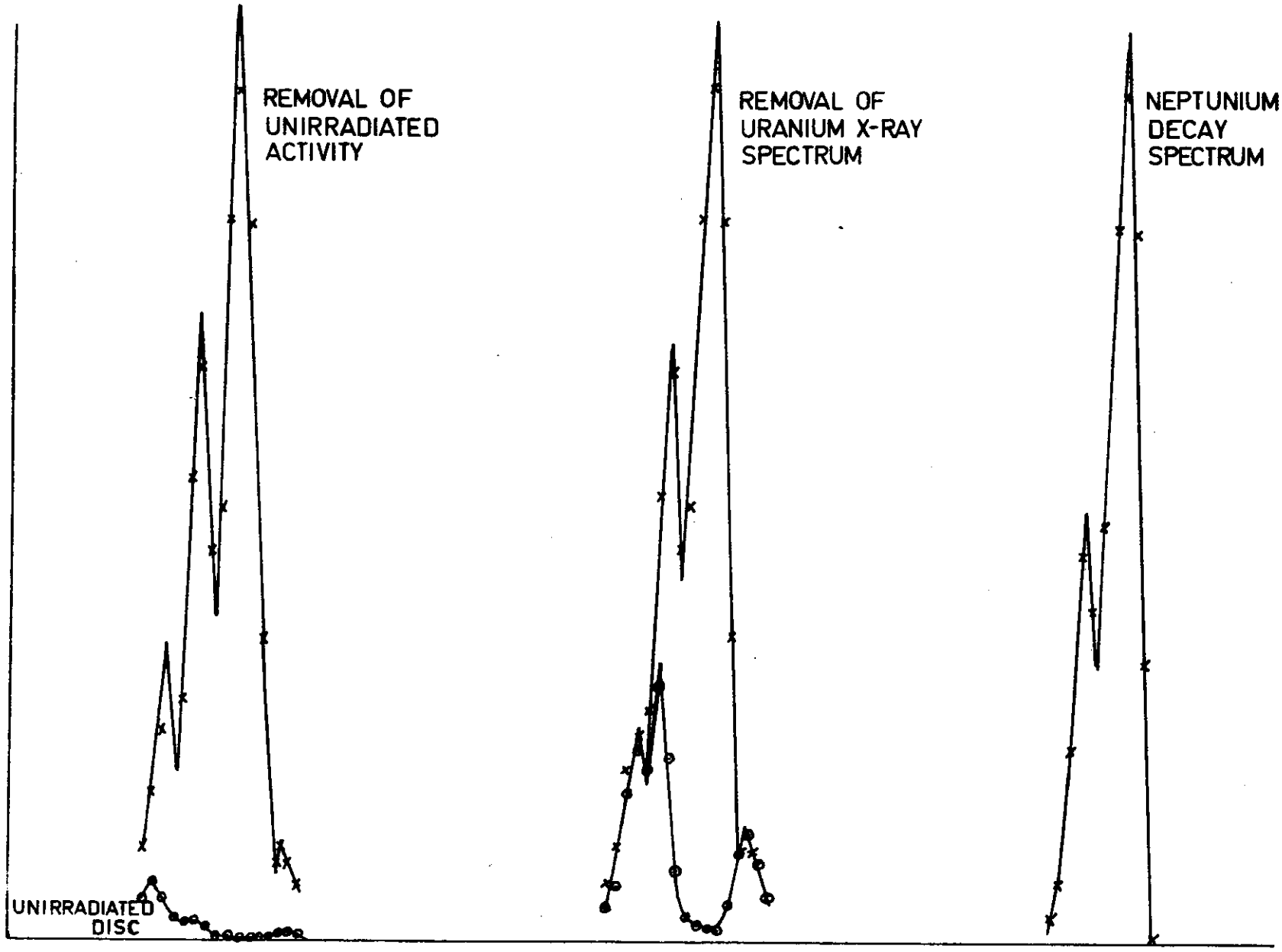

FIGURE 17. THE ANALYSIS OF THE NEPTUNIUM ACTIVITY

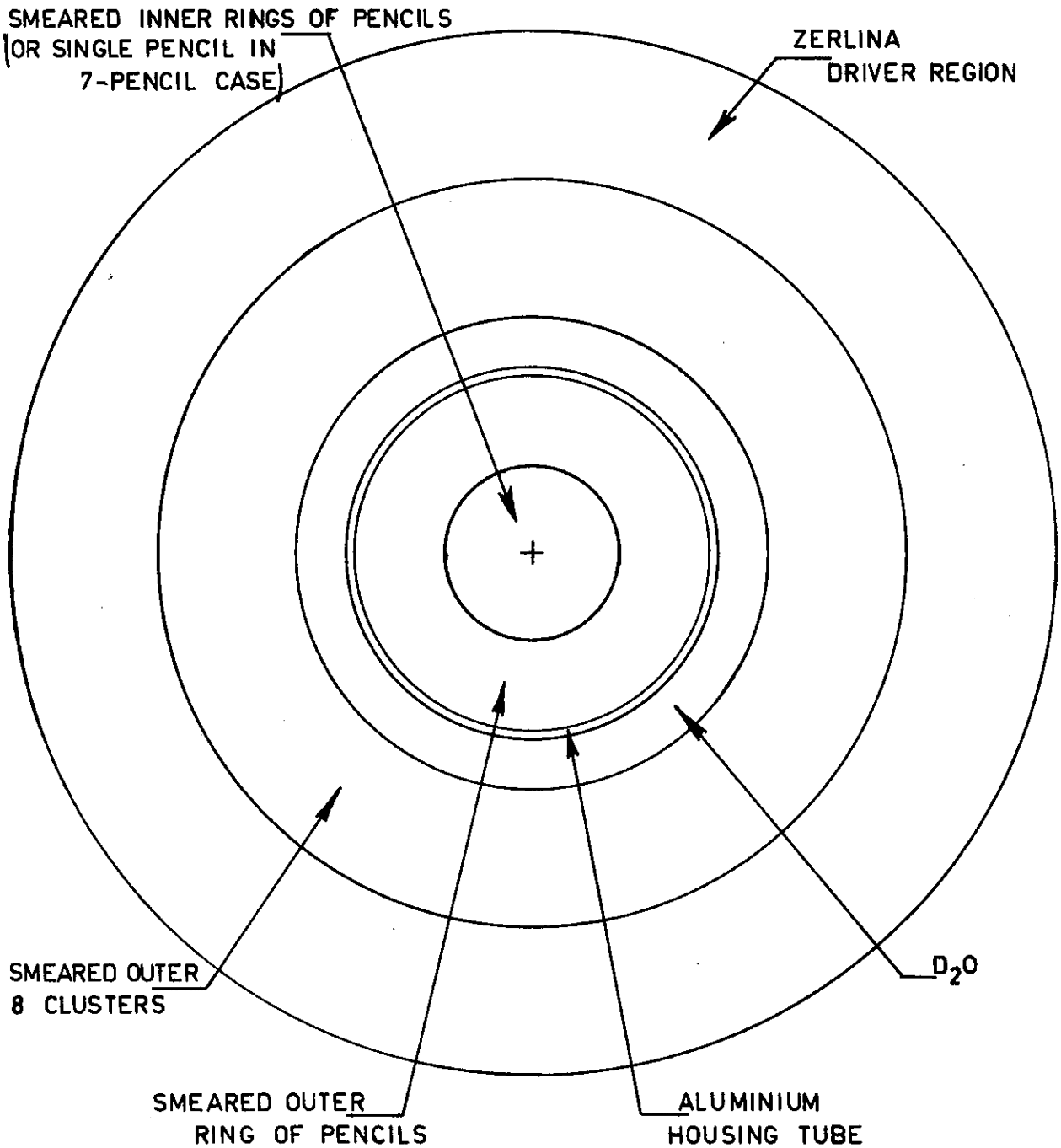

FIGURE 18. GENERAL ARRANGEMENT OF REGIONS USED IN THE REPRESENTATION OF ZERLINA